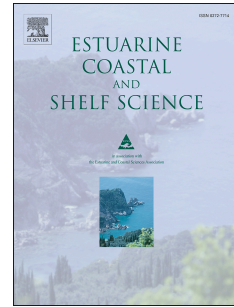


Accepted Manuscript

Habitat mapping of the Maltese continental shelf using acoustic textures and bathymetric analyses

Mariacristina Prampolini, Philippe Blondel, Federica Foglini, Fantina Madricardo



PII: S0272-7714(17)30600-5

DOI: [10.1016/j.ecss.2017.06.002](https://doi.org/10.1016/j.ecss.2017.06.002)

Reference: YECSS 5491

To appear in: *Estuarine, Coastal and Shelf Science*

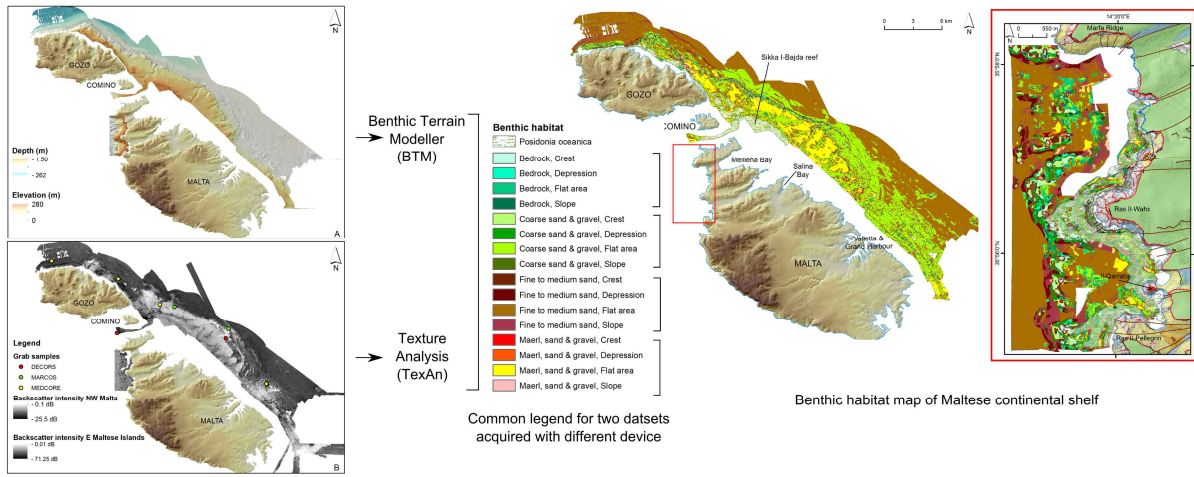
Received Date: 10 May 2016

Revised Date: 19 April 2017

Accepted Date: 2 June 2017

Please cite this article as: Prampolini, M., Blondel, P., Foglini, F., Madricardo, F., Habitat mapping of the Maltese continental shelf using acoustic textures and bathymetric analyses, *Estuarine, Coastal and Shelf Science* (2017), doi: 10.1016/j.ecss.2017.06.002.

This is a PDF file of an unedited manuscript that has been accepted for publication. As a service to our customers we are providing this early version of the manuscript. The manuscript will undergo copyediting, typesetting, and review of the resulting proof before it is published in its final form. Please note that during the production process errors may be discovered which could affect the content, and all legal disclaimers that apply to the journal pertain.



ACCEPTED MANUSCRIPT

1 **Habitat mapping of the Maltese continental shelf using acoustic textures** 2 **and bathymetric analyses**

3 Mariacristina Prampolini ^{a,b}, Philippe Blondel ^c, Federica Foglini ^b, Fantina Madricardo ^d

4 ^a Department of Chemical and Geological Sciences, University of Modena and Reggio Emilia, Via Campi
5 103, 41125 Modena (Italy)

6 ^b National Research Council, Institute of Marine Sciences (CNR-ISMAR), Bologna, Via Gobetti 101, 40129
7 Bologna (Italy)

8 ^c Department of Physics, University of Bath, Claverton Down, BA2 7AY Bath (UK)

9 ^d National Research Council, Institute of Marine Sciences (CNR-ISMAR), Venezia, Tesa 104 – Arsenale,
10 Castello 2737/F, 30122 Venezia, (Italy)

11

12 Corresponding author: Mariacristina Prampolini, e-mail: mariacristina.prampolini@unimore.it, Phone: +39
13 059 2058453

14

15 **ABSTRACT**

16 The uneven mapping of the Maltese continental shelf precludes a full assessment of its marine
17 habitats, important for their monitoring and conservation in line with the EU Marine Strategy
18 Framework Directive and local initiatives. From 2009 to 2012, high-resolution multibeam
19 echosounder (MBES) surveys offshore the NW and E coasts of the Maltese archipelago were
20 carried out, covering a total area of 1,408.3 km² with a maximum resolution of 1 m, at depths from
21 1.5 to 263 m. The types of benthic habitats occurring on the continental shelf often showed subtle
22 acoustic variations. This article aims at 1) integrating analyses of the bathymetry and acoustic
23 textures with ground-truthing (grab samples) in key areas; 2) validating this combined approach by
24 rewriting an existing benthic habitat map of the eastern continental shelf of Malta; 3) exploiting this
25 ground-truthed classification to calibrate an unsupervised classification of a dataset acquired with a

26 different sonar. The main results obtained from these analyses are i) a sediment map of the
27 continental shelf of NW Malta and east of the Maltese archipelago – classifying in detail bedrock,
28 rocky blocks, coarse sand and gravel, fine to medium sand and maërl, sand and gravel – that
29 supports the geomorphological interpretation of the seabed features; ii) an automatic classification
30 of the seafloor morphology, highlighting a very gentle sloping seabed crossed by the shelf break
31 and by palaeo-river valleys; iii) the first full benthic habitat map of the continental shelf offshore E
32 and NW coast of Malta obtained with a semi-automatic classification. In this work, we highlight and
33 explain the main differences in seafloor sediment coverage, its morphology and the relative
34 occurrences of benthic habitats between the NW and E sides of the Maltese archipelago.

35

36 **KEYWORDS:** Seafloor classification; Marine sediments; Acoustic textures; Benthic habitat; Malta

37

38 1. INTRODUCTION

39 Shallow waters host the most complex mosaic of benthic habitats, making them the most
40 productive marine environments (Eyre and Maher, 2011; Gray, 1997). Increasingly, anthropogenic
41 activities are concentrating along the coasts, in shallow waters in particular. They include fishing
42 (comprising trawl fishing), aquaculture, harbour and shipping activities, mineral exploration and
43 exploitation, and offshore construction (e.g. for marine renewable energy, like wind farms). These
44 activities all have potentially important impacts on the marine environments and habitats, which
45 need to be monitored and controlled. The knowledge of marine ecosystems spatial distribution and
46 their quality is fundamental to protect them from anthropogenic actions (Jackson et al., 2001).
47 Thus, habitat maps are a necessary tool for marine environmental assessment and management,
48 protection of valuable habitats, hazards assessment and monitoring human activities.

49 There are many approaches to benthic habitat mapping, depending on the type of acoustic data
50 and its spatial resolution, the types and varieties of habitats under investigation, the size of the
51 datasets and the quality of any ancillary information available (from ground samples to video

52 transects of sub-bottom profiles). For a rapid view of the current state of the field, the reader is
53 directed toward the more recent articles of Brown and Blondel (2009), Brown et al. (2011),
54 Ierodiaconou et al. (2011), Lucieer and Lamarche (2011), Micallef et al. (2012), Diesing et al.
55 (2014), McGonigle and Collier (2014) and Montereale Gavazzi et al. (2016) and references therein.
56 It is possible to apply a single method or to combine several (e.g. hybrid approaches, multi-method
57 ensembles) as suggested by Diesing et al. (2014) or Montereale Gavazzi et al. (2016). This
58 second approach has been repeatedly shown as the most effective way to improve any kind of
59 classification since the final seabed classification is supported by more than one analysis (Erdey-
60 Heydorn, 2008; Wright and Heyman, 2008; Marsh and Brown, 2009; Lamarche et al., 2011;
61 Micallef et al., 2012).

62 These different procedures can use automatic or manual classification of the data. Automatic
63 classification uses either signal-analysis or image-analysis methods: the latter can be applied to
64 data acquired with different instruments, and both methods are repeatable, quantitative and
65 objective – as suggested by Diesing et al. (2014) – allowing to process large amounts of data
66 faster. Signal-based analyses are associated to individual measurements, at the level of the
67 backscatter value, whereas image-based ones better described the larger-scale organisations of
68 seafloor substrate and benthic habitats. Again, there is a plethora of approaches developed
69 specifically for sonar measurements. These include Principal-Components Analyses of multiple
70 attributes within proprietary software packages, e.g. QTC-Sideview (Preston et al., 2000;
71 McGonigle et al., 2009; Preston, 2009); artificial neural network techniques (Marsh & Brown,
72 2009); Bayesian decision rules (Simons & Snellen, 2009); decision trees (Dartnell and Gardner,
73 2004; Rooper and Zimmermann, 2007; Rattray et al., 2009; Ierodiaconou et al., 2011; Che Hasan
74 et al., 2012a); support vector machines (Che Hasan et al., 2012b); Random Forest (Che Hasan et
75 al., 2012b; Lucieer et al., 2013); Maximum Likelihood Classifier (Buhl-Mortensen et al., 2009;
76 Ierodiaconou et al., 2011; Che Hasan et al., 2012b); Texture Analysis (Blondel, 1996; Blondel et al.,
77 1998; Gao et al., 1998; Huvenne et al., 2002; Cochrane and Lafferty, 2002; Gómez Sichi et al.,
78 2005; Huvenne et al., 2007; Blondel and Gómez Sichi, 2009).

79 The Mediterranean Sea represents an ideal natural laboratory for benthic habitat mapping and
80 monitoring due to: i) its complex geological setting and seafloor geomorphology; ii) high diversity of
81 its important ecosystems; iii) high density of human activities impacting on seafloors and habitats.
82 The Maltese seafloors in particular host habitats of high ecological value, going from white, red and
83 black corals (Deidun et al. 2010) to seagrass meadows and maërl beds (Borg et al., 1998, 2005,
84 2009; Galdies and Borg, 2006; Sciberras et al., 2009). They are often located in touristic areas,
85 close to harbour zones and fisheries, and part of these habitats are recognized as marine Natura
86 2000 sites.

87 The present study focuses on the Maltese archipelago and its marine habitats, presented in
88 Section 2. The Materials and Methods are explained in Section 3, showing the different types of
89 acoustic measurements and supporting data (grab samples in representative locations) that we
90 collected, along with recent information on marine habitats from the Malta Environment and
91 Planning Authority (MEPA; Borg et al., 1998, 2005, 2009; Scieberras et al., 2009). The first
92 objective is to outline a quantitative, repeatable, automatic or semi-automatic procedure to map the
93 distribution of benthic habitats around Malta. The large amounts of high-resolution acoustic data
94 (bathymetry and backscatter), in two different locations (E and NW continental shelves of the
95 Maltese archipelago) and with different echosounders, justify the need for image-based
96 approaches, namely the automatic analysis of seafloor morphology (Section 3.2) and semi-
97 automatic classification of backscatter with Textural Analysis (Section 3.3). The second objective of
98 this study is to extend an existing and ground-truthed classification (Micallef et al., 2013) to an
99 adjacent dataset where no seafloor samples are available. These results are presented for each
100 region individually (Section 4). Thus, we present a single benthic habitat classification for two
101 adjacent datasets acquired with different devices. The differences in habitat distributions between
102 the E and NW sides of the Maltese archipelago are analysed in Section 5, compared to each other
103 and to previous works in neighbouring areas, showing the synergy between approaches and
104 contributing to the knowledge of the marine habitats around Malta at depths ranging from 1.5
105 (immediate near-shore) to 263 m (continental break).

106 **2. STUDY AREA**

107 The Maltese archipelago is located in the Sicily Channel on the Malta Plateau and comprises the
108 islands of Malta, Gozo and Comino. An Oligocene-Miocene succession made up of mainly
109 carbonatic formations (Pedley et al., 2002) characterises the geological setting of the archipelago
110 (Fig. 1): (a) Lower Coralline Limestone Formation; (b) Globigerina Limestone Formation; (c) Blue
111 Clay Formation; (d) Upper Coralline Limestone Formation. The whole succession slopes 4°
112 towards NE because of the uplift and tilting due to the location of the archipelago on a shoulder of
113 the Malta Graben (part of the Pantelleria Rift system; Pedley et al., 2002). The islands are also
114 affected by two fault systems: the WSW-ENE-oriented system is the oldest one and its major
115 lineament is the Great Fault; the NW-SE-oriented system is the most recent one, parallel to the
116 Pantelleria Rift, and its major fault is the Maghlaq Fault (Dart et al., 1993; Putz-Perrier and
117 Sanderson, 2010). This tectonic setting and the superimposition of lithologies with different
118 mechanical behaviour and resistance to erosion are the main agents controlling the land- and
119 seascape.

120 The geomorphology of the Island of Malta has been largely investigated by Alexander (1988),
121 Magri (2006), Devoto et al. (2012), Mantovani et al. (2013), Biolchi et al. (2016). The Maltese
122 landscape is tectonically and lithologically controlled and modelled by marine action processes,
123 karst, fluvial and gravity-induced processes. The ENE-WSW fault system is responsible for the
124 *horst-and-graben* structure both at small and large scale (Dart et al., 1993), especially in the area
125 north of the Great Fault. The NW-SE fault system controls the trend of the northern and southern
126 coasts of the islands. Generally, on the E side of the archipelago, low-lying coasts occur (i.e.
127 sloping coasts and shore platforms), while plunging cliffs and boulder screes characterise the
128 western and southern coasts of the islands. Screes are widespread, especially along the NW coast
129 of Malta, and are due to the development of mass movements, mainly block slides. The latter
130 involve the Upper Coralline Limestone plateaus and the underlying Blue Clay terrains: limestone
131 blocks detached from the carbonate plateaus and slide downhill over the clayey slopes. Rock fall
132 and superficial earth flow/slides are common processes too. Also karst processes are widespread,

133 creating karst pavements, speleothems, caves, dolines and sinkholes (Pedley et al., 2002; Galve
134 et al., 2015). Due to the 4°-tilting toward NE, the hydrography developed with a SW-NE orientation,
135 with river valleys and temporary water streams (named *wied* in Maltese).

136 Preliminary results about the morphological features and evolution of the continental shelf of the
137 Maltese archipelago were presented by Micallef et al. (2013) and Foglini et al. (2016). The
138 differences in landscape between the E and NW areas of Malta observable on land are reflected
139 on the seafloor. On the E side of the islands, there is a wide and almost flat continental shelf,
140 bordered by an escarpment parallel to the present-day coast and crossed by the submerged
141 prolongations of the river valleys. Karst features and marine terraces are also present. On the NW
142 side of Malta, the continental shelf is very narrow and fragmented and the escarpment is
143 constituted by subvertical cliffs and marine terraces; the main landforms of the shelf are given by
144 the submarine extension of the coastal landslides resulting in large accumulations of rocky blocks.

145 The marine habitats of the Maltese seafloor are characterised by the presence of white corals
146 deeper than 400 m, red and black corals at intermediate depths (Deidun et al. 2010), seagrass
147 meadows in the infralittoral zone and maërl in the circalittoral zone (Borg et al., 1998, 2005, 2009;
148 Galdies and Borg, 2006; Sciberras et al., 2009). The prevailing occurrence of red coral on the
149 seafloor offshore the NW coasts of the Maltese Islands, as recorded by Deidun et al. (2010), might
150 be attributed to the seabed morphology and composition (mainly rocky with pockets of
151 coralligenous biocoenosis), the sea currents chiefly from the NW and the restriction of the
152 continental shelf causing an abrupt increase in sea depth, forming submarine cliffs and vertical
153 walls.

154 The dominant benthic habitats in shallow waters, and mainly offshore the E coasts of the
155 archipelago, are sandy bottoms with seagrass meadows (*Posidonia oceanica* and *Cymodocea*
156 *nodosa*); at 40 m and even deeper, bare sands occur with seagrass meadows; the circalittoral
157 zone is characterised by a strip of *maërl* and then fine sediments at 80 m and deeper (Borg et al.,
158 1998). In particular, Borg et al. (2009) described the types of bed on which *P. oceanica* could be
159 settled. From shallow to deep water, they vary from small patches of *P. oceanica* on rocky

160 substratum, to reticulate beds settled on soft sediment interspersed with bare sand, continuous
161 and/or reticulate beds on matte and finally both reticulate or patches of *P. oceanica*. The
162 abundance of seagrass meadows on the Maltese seafloors can be attributed to water clarity with
163 no eutrophication, due to the absence of permanent hydrography, and can also be influenced by
164 the submarine geomorphology and the hydrodynamic conditions of the area (Drago, 1999).

165 Deeper than 44 m, *P. oceanica* and *Cymodocea nodosa* habitats are replaced by the occurrence of
166 *maërl*, a type of benthic habitat characterised by a high diversity of associated macrobenthos (Borg
167 et al., 1998; Sciberras et al., 2009). It is formed by accumulations of calcareous rhodophytes
168 forming a rhodolith-like shape and, in the NW Mediterranean, it can occur down to 65 m deep
169 (Pérès, 1985). On the seafloor offshore the E Maltese coasts, a small patch of relict *maërl* was first
170 found in 1994 at a depth of 42 m offshore the Island of Comino, as confirmed by Borg et al. (1998).
171 Sciberras et al. (2009) characterised the species occurrence in Maltese *maërl*. It has been found at
172 depths of ca. 40 – 100 m, in particular the rocky shoal of Sikka Il-Bajda (off Mellieha Bay) is
173 covered by beds extending north-eastward offshore Gozo.

174

175 3. MATERIALS AND METHODS

176 3.1 Data

177 The datasets analysed were collected offshore the E coasts of the Maltese archipelago and
178 offshore the NW coast of the Island of Malta, north of the Great Fault (Fig. 1).

179 The E dataset (offshore from north Gozo to south-east Malta – 1,390 km²) was acquired with a
180 Kongsberg multibeam echosounder (MBES) EM710 (70-100 kHz) installed on board the R/V
181 Urania of the CNR (Italy). In this area, grab samples of the seafloor were also collected (Fig. 2).
182 Bathymetric and backscatter data offshore the NW coast of Malta (from Marfa Ridge to Ras Il-
183 Pellegrin promontory – 18.53 km²) were acquired with the wide swath sonar system SWATHplus-L
184 (117 kHz) installed on board the Isis II catamaran of the AquaBioTech Group. High-resolution
185 bathymetry (2-m resolution seafloor DEM; Fig. 1) and backscatter data (1-m resolution for the NW

186 dataset and 2-m resolution for the E dataset) of the Maltese continental shelf were processed
187 using CARIS HIPS and SIPS, in order to analyse the seafloor geomorphology and the backscatter
188 image.

189 Data on the distribution of *Posidonia oceanica* on the Maltese seafloors are available from MEPA
190 and have been published by Borg et al. (1998, 2005, 2009) and Sciberras et al. (2009). This
191 biological information will be overlaid on the final maps resulting from the combination between the
192 geomorphological and backscatter texture analyses.

193

194 **3.2 Morphological classification**

195 In the present work, a morphometric analysis of the Maltese seafloor was carried out in order to
196 produce an automatic seafloor morphological classification into crests, depressions, slopes and flat
197 areas. The morphometric analysis was performed using the Benthic Terrain Modeller (BTM)
198 toolbox implemented for ArcGIS 10.x (Wright et al., 2005; Lundbland et al., 2006). This toolbox is
199 made of several functions that allow to calculate environmental variables, such as Bathymetric
200 Position Index (BPI) and standardised BPI that will be defined below. Among these tools, we used
201 the Zone Classification Builder which is a codified flow chart that automatically classifies seafloor
202 morphology combining the properties of slope, Bathymetric Position Index (BPI; the same as
203 Topographic Position Index described by Wright and Heyman, 2008 and Jenness et al., 2011) and
204 standardised BPI (calculated in order to overcome scale-dependency of BPI data, as suggested by
205 Verfallie et al., 2007). In Zone Classification Builder, we were asked to manually set a slope
206 threshold to distinguish between gentle and steep slopes: we selected the value of 5° in order to
207 highlight also subtle variations of the slope. Then, the variables derived from the bathymetric DEM
208 and the selected parameter were combined to identify distinct seafloor morphometric regions..

209 The resulting seafloor morphological classification is presented in Fig. 2, where we extracted four
210 classes: crests, depressions, flat areas and slope.

211

212 3.3 Backscatter Texture Analysis

213 The decision to apply TexAn Texture Analysis to the Maltese datasets instead of any other
214 methodology was motivated by the following factors:

- 215 i. it is an image-based segmentation method and a feature-based approach: it identifies
216 acoustic patterns and specific features at the local or regional level. An image-based
217 segmentation can be applied to different datasets giving comparable results, as in this
218 work. Moreover, the analysis of acoustic patterns typical of specific features is the best way
219 to describe the seafloor substrate, since the analysis of the backscatter signal would have
220 been a partial characterisation of the seafloor due to the occurrence of features with the
221 same signal or more signals for the same features according to the variation of grazing
222 angle.
- 223 ii. it identifies textures not distinguishable by human eye, making the classification more
224 objective (Blondel, 1996);
- 225 iii. it is based on Grey Level Co-occurrence Matrices (GLCMs) that have been proved to be
226 the most adaptable tools for textural analyses of sonar imagery (Blondel, 1996; Gao et al.,
227 1998; Micallef et al., 2012);
- 228 iv. it is not influenced by depth, data acquisition choices and variation in pulses lengths during
229 the acquisition: along with the adequate processing performed with CARIS software, any
230 variations at very large scales would be ignored by the localised texture analyses (Blondel
231 et al., 2015). The individual acoustic responses from seabed patches are combined into
232 MBES pixels, 1-m² in this case. They are modulated by the spatial scale at which the
233 seabed changes, which can be smaller or larger than 1 m, and by the amount of acoustic
234 penetration into the seabed (estimated at centimetres for the frequencies used here). Their
235 variations are best expressed as textures, and the TexAn software (Blondel, 1996) has
236 been used successfully to identify and quantify subtle acoustic patterns in sidescan sonar
237 imagery (e.g. Huvenne et al., 2002) and in MBES imagery (e.g. Blondel and Gómez Sichi,

238 2009), in particular for similar terrains in the coastal regions of Malta (Micallef et al., 2012),
239 and to relate them to specific habitats, validated with ground-truthing;

240 v. two benthic habitat maps are already available for the dataset located offshore the E coasts
241 of the Maltese archipelago. The first one was performed by Micallef et al. (2012) for a
242 portion of the seafloor located in coastal waters (6-57 m deep), between Marfa Ridge and
243 Salina Bay (see Fig. 1B in Micallef et al., 2012), that is not comprised in the dataset
244 analysed here. A more recent classification of the entire E dataset was produced by Micallef
245 et al. (2013). We decided to apply the same approach that they used in the previous works:
246 a combination of morphometric classification with textural analysis of the backscatter image
247 to produce a ground-truthed benthic habitat map. This decision was motivated by the fact
248 that we wanted to reproduce the same classification for the E dataset in order to extend it to
249 the NW dataset that cannot rely on seabed samples and was acquired with an
250 interferometric system, different from the MBE used for the E dataset.

251 Textures are quantified by the co-occurrence of identical grey levels at specific distances from each
252 other, within computation windows of a size commensurate to the morphological processes of
253 interest. The full details are given in Blondel (1996), Blondel and Gómez Sichi (2009) and Micallef
254 et al., (2012) *inter alia*, and they will not be repeated here. MBES backscatter imagery expressed
255 pixels as calibrated dB values: they are initially resampled to 8-bit grey levels, yielding resolutions
256 of ca. 0.3 dB and 0.1 dB per grey level, for the E and NW datasets respectively. Quantified over a
257 specific number of grey levels (noted NG , decreasing from 256 down to 8 by factors of 2), this high
258 radiometric resolution should allow distinguishing the more subtle variations in textural patterns.
259 These are quantified using the indices of entropy and homogeneity, calculated over windows of
260 different sizes (noted $WDSZ$, varying from 60 down to 10 pixels square by steps of 5 pixels) and for
261 inter-pixel displacements (noted SZ) from slightly less than the window size down to 5 pixels, again
262 by steps of 5 pixels.

263 In order to classify the backscatter image for the different type of substrate, it is necessary to select
264 Training Zones, areas representative of the main acoustic facies within each dataset. They are

265 used to train the model in the identification and separation of the acoustic patterns representative
266 of each type of seafloor substrate. Training Zones need to be small enough to incorporate only one
267 type of facies, if possible, but they also need to be large enough that they yield enough textural
268 signatures (entropy/homogeneity pairs) to be statistically significant. For the E dataset, Training
269 Zones of 80×80 pixels (i.e. 160×160 m on the ground) were used to define 10 Training Zones,
270 further identified with grab samples (Fig. 3A; Table A1). The selection of Training Zones centred on
271 the location of grab samples allow an automatic ground-truthing of the classification for the E
272 dataset. For the NW dataset, they were chosen as 82×82 pixels (i.e. 82×82 m on the ground),
273 and 12 different Training Zones were selected (Fig. 3B; Table A2).

274 After the selection of the Training Zones, GLCMs were calculated for these selected areas,
275 averaged over all orientations possible, using different values of the number of grey levels NG, the
276 extent of the area over which their textures are distinct enough (WDSZ) and the intrinsic scale at
277 which these changes occur (SZ). At this stage, it is necessary to identify the optimal combination of
278 NG, WDSZ and SZ that better separate the Training Zones within the diagram. The indices
279 reported on the horizontal and vertical axes are entropy and homogeneity: the best textural indices
280 to be applied for seafloor backscatter image classification, as evaluated by Blondel (1996) and
281 later confirmed by Gao et al. (1998) or Cochrane and Lafferty (2002). Entropy is higher for rougher
282 textures, lower for smoother or more organized textures. Conversely, homogeneity quantifies the
283 amount of local similarities (it is also called inverse-difference moment by some authors; see
284 Blondel, 1996). The inverse scale used in TexAn means it is lower for more organised textures,
285 and higher as textures include more heterogeneous objects, e.g. blocks within a smooth
286 background.

287 For the E dataset, the optimal separation between Training Zones was found for NG = 64 grey
288 levels, WDSZ = 50 pixels and SZ = 5 pixels. This means that, based on their textures, the different
289 regions were best distinguished if looking at differences of more than 1 dB, over scales of 10 m but
290 within ranges less than 100 m. The progression in entropy and homogeneity is associated with
291 increasing grain sizes. The parts covered by fine to medium sand and the more homogeneous

292 areas have lower entropies and homogeneities (Fig. 4). Both textural signatures increase for
293 coarse sand (slightly rougher but less homogenised), coarse sand, gravel and blocks of calcarenite
294 (rougher textures at this scale, with local organisation but no organisation visible at scales close to
295 60 m).

296 For the NW dataset, TexAn found an optimal separation between Training Zones (Fig. 4) for $NG =$
297 64 grey levels, $WDSZ = 60$ pixels and $SZ = 5$ pixels. This means that, based on their textures, the
298 different regions are best distinguished if looking at differences of more than 0.4 dB (the full
299 radiometric range of 25.5 dB, Fig. 3, resampled onto 64 grey levels), over scales of 5 m but within
300 ranges of less than 60 m. These values are comparable with those of the E dataset.

301 The textural parameters identified as optimal for the E dataset are then used to process the entire
302 E backscatter mosaic, producing one image of entropy and one image of homogeneity, co-located
303 and at the same resolution as the backscatter image (Fig. A1 for E dataset and Fig. A2 for NW
304 dataset). These images are clustered using K-means, as presented in Blondel and Gómez Sichi
305 (2009), in order to get an objective combination of entropy and homogeneity within the dataset.
306 This simple partitioning scheme (Duda and Hart, 1973) results in mutually exclusive clusters of
307 entropy/homogeneity signatures, recursively adapted until convergence. The initial number of
308 classes is generally chosen as slightly higher than the number of acoustic *facies* expected,
309 allowing provision for “mixed” classes, “unexpected classes” etc. (Blondel and Gómez Sichi, 2009).
310 Through K-means, we combined the entropy and homogeneity maps to produce a map of 20
311 classes for the E dataset of Malta. Then, user-led contextual editing allows re-assigning clusters to
312 physically meaningful processes such as habitats and morphologies, guided by any ground truth or
313 other available measurements. The final sediment classification highlights the occurrence of 4
314 types of seabed sediments: bedrock; coarse sand and gravel; maërl, sand and gravel; fine to
315 medium sand (see Fig. 5). The same procedure was conducted on the NW dataset, allowing to
316 produce a map of seafloor sediments including the same classes of the E dataset and adding the
317 class rocky blocks (Fig. 6). Thus the two datasets have a common legend for the seafloor
318 sediments distribution.

319 4. RESULTS

320 4.1 E Malta dataset

321 The seafloor offshore the E coasts of the Maltese archipelago is flat or almost flat from the coastal
322 waters (1.5 – 2-m deep) to the basin area. The main seafloor feature is the shelf break dividing the
323 continental shelf from the basin area and well highlighted in the BTM morphological classification,
324 where it is represented as a crest (Fig. 2). The main feature of the basin area is an elongated
325 mound drift due to contouritic currents (Micallef et al., 2013), located just downslope the
326 escarpment and extending from NE Gozo to Comino. It has a very gentle slope, thus only the
327 external boundary of this deposit is classified as crest and slope, while the rest of this feature is
328 classified as flat areas. The shelf break and the breaks of slope of the marine terraces are
329 classified as crests, while the cliffs of the escarpments are classified as slopes. The occurrence of
330 the channels crossing the continental shelf in direction SW-NE and interpreted as palaeo-river
331 valleys by Micallef et al. (2013) and Foglini et al. (2016) area highlighted by the BTM classification,
332 especially in their final part, the mouth cutting the continental escarpment. According to their
333 inclinations, the lateral walls of the channels are classified as crests or slopes. In shallow waters,
334 offshore Mellieha Bay, in the Comino Channel and in front of Comino, there are slightly elevated
335 plateau-like areas showing an irregular, rough surface. The largest of these areas is Sikka l-Bajda,
336 a bedrock reef identified as a potential offshore wind farm location (as reported in the Global
337 Offshore Wind Farm Database; Micallef et al., 2013). In the southern part, from Sliema to south of
338 Valletta, features parallel to each other, and interpreted by Micallef et al. (2013) and Foglini et al.
339 (2016) as palaeo-shoreline deposits formed during the post-glacial sea level rise are classified as
340 crests.

341 Through K-means, we obtained the seafloor sediment map shown in Fig. 5, where the geological
342 map of the Maltese archipelago is reported, so that we can relate the Texan sediment map of the
343 seafloor to the geology on land. The seafloor located downslope the escarpment is principally
344 characterised by an almost flat and smooth seafloor with low backscatter intensity, except for the
345 southern area where some parts of high intensity are scattered across the seafloor. The habitat

346 map classified this deeper area as flat seafloor, mainly covered by fine to medium sand and with
347 some scattered bedrock outcrops in its southern sector, highlighted both in the morphological and
348 sediment maps.

349 On the continental shelf, both the morphology and the sediment coverage vary considerably:
350 generally, the seafloor is almost flat and characterised by some bedrock outcrops in positive relief
351 and by channels crossing the shelf with an orientation NW-SE. The seabed is mainly constituted by
352 coarse sand and gravel, often the substrate is characterised by wide *maërl* beds. The presence of
353 finer sediment is primarily located within the channels, whose bottom is characterised by ripples.
354 Fine to medium sand is alternated with coarse sand and gravel in a shallow area offshore Comino
355 Island, in correspondence of a meandered channel, where the seafloor is almost flat, smooth and
356 slightly lowered with respect to the surrounding bedrock outcrops. It is interpreted as a palaeo-
357 alluvial plain filled by mobile sediment and characterised by lobes and ripples.

358 The seafloor located in front of Valletta and the Grand Harbour shows a very singular acoustic
359 pattern highlighted through the entropy and homogeneity maps: in a flat area, that is supposed to
360 be covered by fine sediment since it is situated at the mouth of an important hydrographic network,
361 a number of high intensity “dots” are scattered over a low backscatter matrix. It was classified as a
362 great variety of sediments covering the seafloor: medium to fine sand alternated with small bedrock
363 outcrops and coarse sand and gravel with the presence of blocks of calcarenite (Fig. 5B). This is
364 due to the human activities that highly disturbed the seafloor integrity, resulting in an area exploited
365 for dumping, excavating and trawling activities (Micallef et al., 2013; Foglini et al., 2016).

366 We combined the BTM morphological classification with the Texan sediment map through the tool
367 Combine of ArcGIS (Spatial Analyst toolset): we produced the final map showing 16 types of
368 seafloor substrate, on which we overlaid the biological data on *Posidonia oceanica* by MEPA (Fig.
369 7). The richest area in *Posidonia oceanica* and *maërl* is the continental shelf. There, the *P.*
370 *oceanica* occurs up to a depth of about 50 m and is settled on bedrock or coarse sand and gravel
371 substrate. The largest *P. oceanica* bed is located on the Sikka Il-Bajda reef, offshore Mellieha Bay
372 and the Island of Comino. The *maërl* distribution confirmed by the only one sample reporting the

373 occurrence of *maërl* bed at a depth of 102 m, offshore Salina Bay (sample DECORS47 from one of
374 our surveys) agrees with the records by Borg et al. (1998) and Sciberras et al. (2009).

375

376 **4.2 NW Malta dataset**

377 The continental shelf offshore the NW coast of Malta is flat or gentle sloping and bounded offshore
378 by the shelf break, classified as crest in the BTM classification (Fig. 2). From coastal waters to ca.
379 50 m deep, the shelf is characterised by an irregular surface with crests, slopes and depressions of
380 limited extension alternated with almost flat and smooth areas. These features are located
381 especially in correspondence of the headlands of Bajda Ridge, Il-Qarraba and Ras Il-Pellegrin and
382 also on the seafloor close to the coast just north of Bajda Ridge and were interpreted as the
383 submerged portion of the landslides affecting the NW coast of Malta (Foglini et al., 2016). The
384 continental slope is characterised by different levels of marine terraces delimited by breaks of
385 slope are classified as crests; while the cliffs constituting the escarpments are recorded as slopes
386 with depressed areas at their base. The area located mainly downslope the continental
387 escarpment is almost flat and characterised by the presence of scattered features in positive relief
388 of different size and shape. The most relevant feature is like a plateau 1000 x 210 m offshore
389 Ghadira Bay, at depths of 70-130 m and ENE-WSW-oriented. Its shape is highlighted by the
390 classification of its boundaries as crests, its cliffs as slopes and its top as flat area. The other
391 features are scattered, with almost rounded shapes and ~50 m in diameter.

392 TexAn classification brought to the production of 5 classes seafloor sediment map shown in Fig. 6.
393 The terrestrial geomorphology shown in Fig. 6 comes from an updated and simplified version of the
394 geomorphological map by Devoto et al. (2012) and is inserted here to relate the seafloor sediment
395 map to the terrestrial geology and geomorphology.

396 The area can be considered as divided into two main parts: a very shallow area (maximum depth
397 50 m) and the deeper area (maximum depth 154 m). The latter is mainly characterised by a flat
398 and smooth seafloor where the backscatter is lower than in the shallower area and the TexAn

399 analysis identified a very homogeneous texture for the entire area. This portion of the seafloor is
400 covered by fine to medium sand with scattered small bedrock outcrops. The shallower area is
401 highly diversified both in geomorphology and in sediment coverage.

402 In correspondence of the promontories there are large accumulations of rocky blocks alternated
403 with the outcrops of bedrock and filled by a matrix of coarse sand and gravel. Since the NW coast
404 of Malta is largely affected by block slides (called *rdum* in Maltese; Devoto et al., 2012, 2013)
405 creating wide deposits of large limestone blocks sliding on the clayey terrains towards the sea, the
406 submarine accumulations of rocky blocks constitute the prolongation of the terrestrial mass
407 movements (Foglini et al., 2016) and TexAn succeeded in isolating the acoustic pattern typical of
408 these accumulations from the surrounding bedrock outcrops (see Fig. 4B).

409 In correspondence of inlets in shallow waters (such as Ghadira Bay and Gnejna Bay), there are
410 some *maërl* beds and alternation of sand and gravel, sediments coming from the sandy pocket
411 beaches present on land. For example, the submarine area of Gnejna Bay (in the southern part of
412 the dataset) is a flat and smooth seafloor showing a high variation in sediment type, from rocky
413 blocks to coarse sand and gravel with or without *maërl*.

414 The last step of the analysis is the combination of the maps resulting from BTM and Texan
415 classification through the Combine tool of ArcGIS: we obtained a 20-class substrate map, over
416 which we overlaid the information on *Posidonia oceanica* occurrence, extracted from the MEPA
417 map server (Fig. 8). The area covered by *Posidonia oceanica* is the most extended habitat of this
418 area. The *Posidonia oceanica* is mainly settled on hard substrate (bedrock, rocky blocks) or on
419 matte (Borg et al., 2009) and occurring on the continental shelf up to the continental escarpment.

420

421 5. DISCUSSION

422 This study presents a multi-method approach to map the marine habitats of the continental shelf off
423 the NW coast of Malta and the E coasts of the Maltese Islands, using predominantly MBES
424 bathymetry and backscatter with ground-truthing in selected locations in the E part only.

425 Generally, we can say that TexAn succeeded in isolating the most representative patterns of
426 sedimentary coverage (Collier and Brown, 2005), as proved in past applications (e.g. Blondel and
427 Gómez Sichi, 2009). This is confirmed for the E dataset where the grab samples available were
428 used to define the Training Zones and validate the classification. A benthic habitat map of the E
429 continental shelf of Malta was already provided by Micallef et al. (2012, 2013). Micallef et al. (2012)
430 focused on a small area in shallow water along the E coast of the Island of Malta, adjacent but not
431 overlapping with the zone analysed in the present work. Micallef et al. (2013) extended the same
432 methodology used in the 2012 paper to the whole E dataset. We reproduced the classification
433 applying their same methodology, but identifying different training zones. On the whole, the results
434 that we obtained are comparable to those produced by Micallef et al. (2012, 2013), with some
435 dissimilarities that could be ascribable to the different processing techniques applied and to the
436 different selection of the Training Zones, the latter playing a key role in our case.

437 The area offshore Valletta and the Grand Harbour is affected by anthropogenic activities that had
438 and still have a large impact on the seafloor. The location and the size of the Training Zones that
439 we selected did not allow the isolation of the pattern typical of spoil ground, apparently at larger
440 spatial scales than the one achievable by the Training Zones. For this reason, the seabed was
441 classified on the basis of the sediment distribution. The inability of isolating this pattern could be
442 considered both as a negative point – since we do not have a “spoil” class in the final map – and
443 as an advantage – since combining our information and the one from Micallef et al. (2013), we
444 know that this portion of seafloor is made of coarse sand and gravel and fine-to-medium sand with
445 blocks of calcarenite, and that this mixture of sediments is due to spoil.

446 Also, the inability in isolating the *Posidonia oceanica* pattern in the present work is mainly caused
447 by the absence of a Training Zone located in the *P. oceanica* meadow. Furthermore, even though
448 the ground samples MEDCOR 51 and 42 (Table A1) recorded the occurrence of *P. oceanica* leaves
449 and rhizomes, Texan was not able to identify its pattern. Micallef et al. (2012) also highlighted this
450 difficulty. In the case of vegetation overlaying a hard substrate, it might be explained by the fact
451 that the acoustic response is predominantly that of the seabed, and only modulated by the

452 vegetation depending on its density, its areal cover within each pixel or groups of pixels, and its
453 intrinsic acoustic reflectivity at the frequencies used (which can vary with photosynthesis or gas
454 content) (e.g. Blondel and Pouliquen, 2004; Kruss et al., 2012). This means that TexAn focused on
455 the key attributes of the substrate but does not appear as good at detecting subtle acoustic
456 modifications if they do not occur over large enough areas.

457 The rationale for the classification of the E dataset was to extend this classification, validated with
458 comparison with ground-truthing dataset, to the NW Malta dataset which was totally lacking
459 ground-truthing. This approach is possible mainly because the TexAn analysis is an image-based
460 segmentation, thus allowing to overcome the fact that the datasets were acquired with different
461 sonar instruments.

462 The differences between the classifications of the E and the NW areas of Malta are shown also in
463 Tables 1 and 2, describing backscatter and bathymetry distributions for each sediment class. The
464 bedrock class in the E dataset is located mainly in correspondence of the continental escarpment,
465 while, on the NW side, bedrock outcrops are widespread at all depths. The class made of coarse
466 sand and gravel is characterised by medium to low values of backscatter and, in the E area, it is
467 quite uniformly distributed down to a depth of 160 m; while on the NW area, it occurs at all depths,
468 with a peak for shallow waters (< 38 m). The sediment class of fine to medium sand has the
469 narrower distribution of backscatter intensity for the E dataset, where it is characterised by low
470 values of backscatter; while in the NW dataset, it is characterised by higher values of backscatter.
471 In both the areas, it is predominant in deeper water. The *maërl* beds are located only on the
472 continental shelf on both the sides of the islands. In the E dataset, they are widespread and
473 present high backscatter intensity, while in the NW area, they have a limited distribution and show
474 medium backscatter intensity. The rocky blocks are present only in the NW dataset, down to a
475 depth of about 40 m and show mainly medium values of backscatter.

476 The E and the NW areas show some differences in sediment distribution that are due to the distinct
477 tectonic and geological settings resulting in a tilt of the archipelago of 4° towards NE that originated
478 a wider continental shelf offshore the E coasts of the islands (continuing the low lying coasts of the

479 E side of Malta) and a narrower continental shelf offshore the NW coast of Malta. The first one is
480 mainly covered by coarse sand and gravel with extensive *maërl* beds; the bedrock outcrops
481 predominantly in correspondence of the continental escarpment and in some scattered reliefs
482 across the dataset, while the deeper area is made of fine and medium sand shaped by bottom
483 currents and contourites. The presence of loose material on the shelf is due both to the temporary
484 streams on land which have their submerged prolongations that acted as channels of sediment
485 transport and to marine sediments deposited during the post-glacial transgression. The NW
486 continental shelf is characterised by coarser and harder sediments: the most significant features
487 are made up by the submarine prolongations of the coastal landslides made up of rocky blocks
488 accumulations, where also bedrock and coarse sand and gravel alternate. The deeper area is flat,
489 smooth and mainly covered by fine and medium sand with some scattered harder outcrops. The
490 most important habitat of the NW area are the *P. oceanica* meadows, while in the E area both *P.*
491 *oceanica* meadows and *maërl* beds occur. This could be due to the difference in sediments and,
492 especially, to the currents: the NW shores of Malta are characterised by high hydrodynamics
493 (Drago, 1999; <http://ioi.research.um.edu.mt/capemalta/stations@malta/INDEX/>), which does not
494 favour the formation of *maërl* biocoenosis.

495 Finally, the advantages of combining data and methods are also discussed by Ierodiaconou et al.
496 (2007), Marsh and Brown (2009) and Che Hasan et al. (2014), who integrated bathymetry and
497 backscatter using different methods. For example, Che Hasan et al. (2014) integrated also analysis
498 of backscatter angular response with that of backscatter image, considering that the contribution of
499 bathymetry represents the most important predictor of marine benthic habitats. They all proved that
500 data integration is more efficient in predicting the benthic habitats than classifications based solely
501 on backscatter or on bathymetry.

502 In the end, the methodology that we propose in this paper could overcome the difficulty of
503 integrating datasets acquired within different cruises, with different instruments and different
504 samples coverage.

506 **6. CONCLUSIONS**

507 The novelty of the present work is that, through a combined approach, we were able to draw a full
508 benthic habitat map of the continental shelf offshore E and NW coast of Malta drawn from a
509 validated dataset (the E one) and then extended to an adjacent dataset – the NW one, acquired
510 with a different device – where no seabed samples were collected.

511 The combined approach applied here is based on the quantitative automatic classification of
512 seafloor morphology with semi-supervised analyses of seafloor backscatter imagery, guided at key
513 points by the biological information already available, either from ground samples or from the
514 MEPA database:

- 515 i. The morphological classification was obtained using the ArcGIS-based tool BTM, different
516 from the technique used by Micallef et al. (2012, 2013), but allowing to extract the same
517 types of quantitative attributes. This kind of analysis can be conducted also through open
518 source software (e.g. GRASS), through additional toolboxes or extensions (e.g. SEXTANTE
519 for QGIS) or through self-built scripting (Lecours et al., 2016 online and references
520 therein). The seafloor features were distinguished in terms of crests, depressions, slopes
521 and flat areas.
- 522 ii. The backscatter mosaics were classified through the TexAn Texture Analysis from which we
523 obtained the sediment distribution map of the seafloor offshore NW Malta and offshore E
524 the Maltese archipelago, distinguishing bedrock, rocky blocks, coarse sand and gravel, fine
525 to medium sand and the occurrence of maërl beds.
- 526 iii. The morphological and the sediment classifications have been combined to obtain a
527 seafloor substrate map. Since, the seagrass pattern was not isolated by TexAn (as it was
528 not clearly visible on the acoustic data), the resulting map has been integrated with existing
529 biological data (from literature and environmental servers) to produce the benthic habitat
530 map of the continental shelf offshore E and NW coast of Malta.

531 We can confirm the reliability of TexAn in classifying the backscatter image, since the sediment
532 distribution map of the seafloor is comparable to those previously produced by Micallef et al. (2012,

533 2013) despite the differences in backscatter processing and the identification of the Training
534 Zones. This kind of automated methods for habitat mapping, reliable also with limited ground-
535 truthing, revealed to be a good and less time-consuming solution to produce seascape maps both
536 at local or regional scale. They offer a valid support to marine resources management, marine
537 spatial planning, habitats monitoring and conservation, usable by Governments and decision
538 makers.

539

540 **ACKNOWLEDGEMENTS**

541 This research is part of the Project “*Coupling terrestrial and marine datasets for coastal hazard*
542 *assessment and risk reduction in changing environments*” funded by the EUR-OPA Major Hazards
543 Agreement of the Council of Europe, 2012-2015 (led by Prof. M. Soldati, Università di Modena e
544 Reggio Emilia). It is also supported by European projects HERMIONE (grant agreement No.
545 226354), COCONET (grant agreement No. 287844) and SCARP (grant agreement No. PCIG13-
546 GA-2013-618149) within the European Community’s 7th Framework Programme (FP7 2007–
547 2013); project PANACEA, (Italy–Malta 2007–2013 Operational Programme I) and project
548 RITMARE (The Italian Research for the Sea) coordinated by the Italian National Research Council
549 and funded by the Italian Ministry of Education, University and Research within the National
550 Research Program (2011–2013). We kindly acknowledge the RPM Nautical Foundation, the
551 captain and crew of R/V Urania of the CNR and of R/V Isis of the ‘AquaBioTech Group’, and
552 Highland Geo Solutions for their assistance with data collection. Part of this research was carried
553 out at the University of Bath (UK) during an exchange in 2014. A subset of the earlier results was
554 presented at conferences EUROGEO 2014 in Malta, GEOHAB 2015 in Salvador (Brazil) and
555 AIGeo 2015 in Cagliari (Italy).

556

557

558

559 REFERENCES

- 560 Alexander, D., 1988. A review of the physical geography of Malta and its significance for tectonic
561 geomorphology. *Quaternary Science Reviews*, 7(1), 41-53.
- 562 Biolchi, S., Furlani, S., Devoto, S., Gauci, R., Castaldini, D., Soldati, M., 2016. Geomorphological
563 identification, classification and spatial distribution of coastal landforms of Malta (Mediterranean
564 Sea). *Journal of Maps*, 12(1), 87-99.
- 565 Blondel, Ph., 1996. Segmentation of the Mid-Atlantic Ridge south of the Azores, based on acoustic
566 classification of TOBI data. In: MacLeod, C. J., Tyler, P. A., Walker, C. L. (eds), Tectonic,
567 Magmatic, Hydrothermal and Biological Segmentation of Mid-Ocean Ridges, *Geological Society,*
568 *London, Special Publications*, 118, 17-28.
- 569 Blondel, Ph., Parson, L. M., Robigou, V., 1998. TexAn: Textural Analysis of sidescan sonar imagery
570 and generic seafloor characterization. In: *Proceeding of the Oceans'98 conference, Piscataway,*
571 *IEEE*, 419–423.
- 572 Blondel, Ph., Gómez Sichi, O., 2009. Textural analyses of multibeam sonar imagery from Stanton
573 Banks, Northern Ireland continental shelf. *Applied Acoustics*, 70, 1288-1297.
- 574 Blondel, Ph, Pouliquen, E. 2004. Acoustic textures and detection of shipwreck cargo – Example of
575 a Roman ship near Elba, Italy In: Akal, T., Ballard, R.D., Bass, G.F. (eds), *Proceeding of First*
576 *Internal Congress on the Application of Recent Advances in Underwater Detection and Survey*
577 *Techniques to Underwater Archaeology, I.N.A., Bodrum, Turkey*, 135-142.
- 578 Blondel, Ph., Prampolini, M., Foglini, F., 2015. Acoustic textures and multibeam mapping of shallow
579 marine habitats – examples from Eastern Malta. In: *Proceedings of the Institute of Acoustics,*
580 *Institute of Acoustic*, 37(1), 250-257.
- 581 Borg, J.A., Howege, H.M., Lanfranco, E., Micallef, S. A., Mifsud, C., Schembri, P. J., 1998. The
582 macrobenthic species of the infralittoral to circalittoral transition zone off the northeastern coast of
583 Malta (central Mediterranean). *Xjenza*, 3(1), 16-24.

- 584 Borg, J. A., Attrill, M. J., Rowden, A. A., Schembri, P. J., Jones, M. B., 2005. Architectural
585 characteristics of two bed types of the seagrass *Posidonia oceanica* over different spatial scales.
586 *Estuarine, Coastal and Shelf Research*, 62, 667-678.
- 587 Borg, J. A., Attrill, M. J., Rowden, A. A., Schembri, P. J., Jones, M. B., 2009. Occurrence and
588 distribution of different bed types of seagrass *Posidonia oceanica* around the Maltese Islands.
589 *Mediterranean Marine Sciences*, 10(2), 45-61.
- 590 Brown, C. J., Blondel, Ph., 2009. Developments in the application of multibeam sonar backscatter
591 for seafloor habitat mapping. *Applied Acoustics*, 70, 1242-1247.
- 592 Brown, C. J., Smith, S. J., Lawton, P., Anderson, J. T., 2011. Benthic habitat mapping: A review of
593 progress towards improved understanding of the spatial ecology of the seafloor using acoustic
594 techniques. *Estuarine, Coastal and Shelf Science*, 92, 502-520.
- 595 Buhl-Mortensen, P., Dolan, M., Buhl-Mortensen, L., 2009. Prediction of benthic biotopes on a
596 Norwegian offshore bank using a combination of multivariate analysis and GIS classification. *ICES*
597 *Journal of Marine Sciences*, 66, 2026-2032.
- 598 Che Hasan, R., Ierodiaconou, D., Laurenson, L., 2012a. Combining angular response classification
599 and backscatter imagery segmentation for benthic biological habitat mapping. *Estuarine and*
600 *Coastal Shelf Science*, 97, 1-9.
- 601 Che Hasan, R., Ierodiaconou, D., Monk, J., 2012b. Evaluation of four supervised learning methods
602 for benthic habitat mapping using backscatter from multi-beam sonar. *Remote Sensing*, 3427–
603 3443.
- 604 Che Hasan, R., Ierodiaconou, D., Laurenson, L., Schimel, A., 2014. Integrating multibeam
605 backscatter angular response, mosaic and bathymetry data for benthic habitat mapping. *PLoS*
606 *ONE*, 9(5), e97339, doi:10.1371/journal.pone.0097339
- 607 Cochrane, G. R., Lafferty, K. D. 2002. Use of acoustic classification of sidescan sonar data for
608 mapping benthic habitat in the Northern Channel Islands, California. *Continental Shelf Research*,

- 609 22(5), 683-690. Collier, J. S., Brown, C. J., 2005. Correlation of sidescan backscatter with grain size
610 distribution of surficial seabed sediments. *Marine Geology*, 214, 431-449.
- 611 Dart, C. J., Bosence, D. W. J., McClay, K. R., 1993. Stratigraphy and structure of the Maltese
612 graben system. *Journal of the Geological Society*, 150(6), 1153-1166.
- 613 Dartnell, P., Gardner, J. V., 2004. Predicting seafloor facies from multibeam bathymetry and
614 backscatter data. *Photogrammetric Engineering and Remote Sensing*, 70, 1081-1091.
- 615 Deidun, A., Tsounis, G., Balzan, F., Micallef, A., 2010. Records of black coral (*Antipatharia*) and red
616 coral (*Corallium rubrum*) fishing activities in the Maltese Islands. *Marine Biodiversity Records*, 3,
617 e90-e96.
- 618 Devoto, S., Biolchi, S., Bruschi, V.M., Furlani, S., Mantovani, M., Piacentini, D., Pasuto, A., Soldati,
619 M., 2012. Geomorphological map of the NW Coast of the Island of Malta (Mediterranean Sea).
620 *Journal of Maps*, 8(1), 33-40.
- 621 Devoto, S., Forte, E., Mantovani, M., Mocnik, A., Pasuto, A., Piacentini, D., Soldati, M., 2013.
622 Integrated monitoring of lateral spreading phenomena along the north-west coast of the Island of
623 Malta. In Margottini, C., Canuti, P. Sassa, K. (eds), *Landslide Science and Practice* (pp. 235-241).
624 Springer Berlin Heidelberg.
- 625 Diaz, R. J., Solan, M., Valente, R. M. 2004. A review of approaches for classifying benthic habitats
626 and evaluating habitat quality. *Journal of Environmental Management*, 73, 165-181.
- 627 Diesing, M., Green, S. L., Stephens, D., Murray Lark, R., Stewart, H. A., and Dove, D., 2014.
628 Mapping seabed sediments: Comparison of manual, geostatistical, object-based image analysis
629 and machine learning approaches. *Continental Shelf Research*, 84, 107-119.
- 630 Drago, A.F., 1999. A study of the sea level variations and the "Milghuba" phenomenon in the
631 coastal waters of the Maltese Islands. PhD dissertation, University of Southampton, UK, p. 432.
- 632 Duda, R.O., P.F. Hart; "Pattern classification and scene analysis", New York: Wiley, 1973.

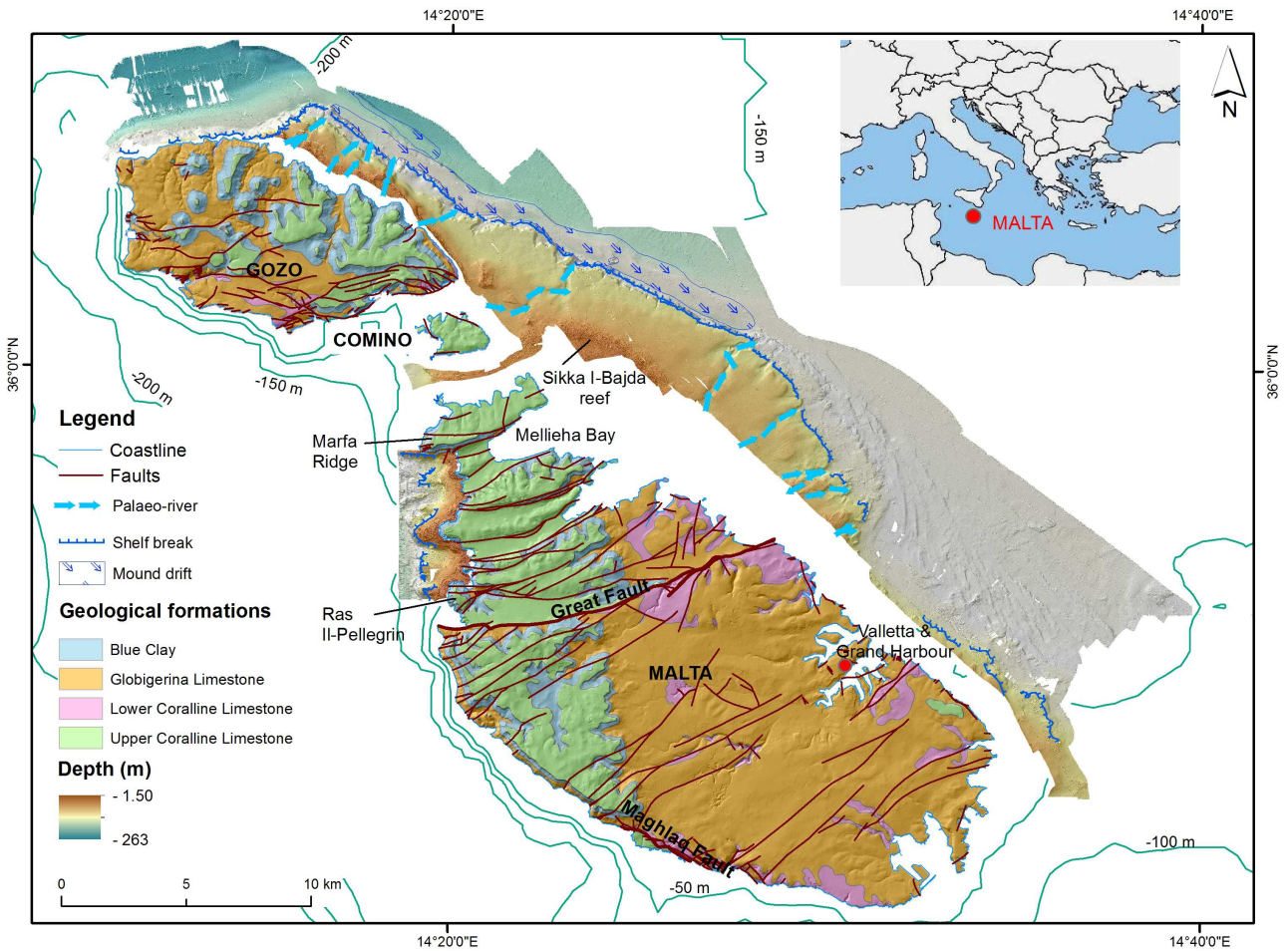
- 633 Erdey-Heydorn, M.D., 2008. An ArcGIS seabed characterization toolbox developed for
634 investigating benthic habitats. *Marine Geodesy*, 31(4), 318-358.
- 635 Eyre, B.D., Maher, D., 2011. Mapping ecosystem processes and function across shallow
636 seascapes. *Continental Shelf Research*, 31, S162–S172.
- 637 Foglini, F., Prampolini, M., Micallef, A., Angeletti, L., Vandelli, V., Deidun, A., Soldati, M., Taviani, M.
638 2016. Late Quaternary coastal landscape morphology and evolution of the Maltese Islands
639 (Mediterranean Sea) reconstructed from high resolution seafloor data. In: Harff J, Bailey G, Lüth F
640 (eds) *Geology and Archaeology: Submerged landscapes of the continental shelf*. Geological
641 Society, London, Special Publications, 411, 77-95.
- 642 Galdies, C., Borg, J.A., 2006. Aerial remote sensing and spatial analysis of marine benthic habitats
643 in St. George's Bay (Malta). 2nd International Conference on the Management of Coastal
644 Recreational Resources
645 Beaches, Yacht Marinas and Coastal Ecotourism – 25-27th October 2006, Gozo, Malta, 81-87.
- 646 Galve, J. P., Tonelli, C., Gutiérrez, F., Lugli, S., Vescogni, A., Soldati, M. 2015. New insights into the
647 genesis of the Miocene collapse structures of the Island of Gozo (Malta, central Mediterranean
648 Sea). *Journal of the Geological Society*, London, 172, 336–348.
- 649 Gao, D., Hurst, S.D., Karson, J.A., Delaney, J.R., Spiess, F.N., 1998. Computer-aided
650 interpretation of side-looking sonar images from the eastern intersection of the Mid-Atlantic Ridge
651 with the Kane Transform. *Journal of Geophysical Research*, 103, 20997-21014.
- 652 Gómez Sichi O., Blondel Ph., Gràcia E. 2005. Acoustic textures and seafloor characterisation of
653 submarine landslides – An example from the SW Iberian Margin. In: Pace N. G. Blondel Ph. (eds),
654 *Boundary Influences in High-Frequency Shallow Water Acoustics*, University of Bath Press,
655 September 2005.
- 656 Gray, J.S., 1997. Marine biodiversity: patterns, threats and conservation needs. *Biodiversity and
657 Conservation*, 6, 153–175.

- 658 Huvenne, V. A. I, Blondel, Ph., Henriet, J.-P. 2002. Textural analysis of sidescan sonar imagery
659 form two mound provinces in the Porcupine Seabight. *Marine Geology*, 189, 323-341.
- 660 Huvenne, V. A. I., Hühnerbach, V., Blondel, Ph., Sichi, O. G., Le Bas, T. 2007. Detailed mapping of
661 shallow-water environments using image texture analysis on sidescan sonar and multibeam
662 backscatter imagery. In: Proceedings of the 2nd Underwater Acoustic Measurements Conference.
663 *Heraklion*: FORTH.
- 664 Ierodiaconou, D., Burq, S., Reston, M., Laurenson, L., 2007. Marine benthic habitat mapping using
665 multibeam data, georeferenced video and image classification techniques in Victoria, Australia.
666 *Journal of Spatial Science*, 52, 93–104.
- 667 Ierodiaconou, D., Monk, J., Rattray, A., Laurenson, L., and Versace, V. L., 2011. Comparison of
668 automated classification techniques for predicting benthic biological communities using
669 hydroacoustics and video observations. *Continental Shelf Research*, 31(2), S28-S38.
- 670 Jackson, J.B.C., Kirby, M.X., Berger, W.H., Bjorndal, K.A., Botsford, L.W., Bourque, B.J., Bradbury,
671 R.H., Cooke, R., Erlandson, J., Estes, J.A., Hughes, T.P., Kidwell, S., Lange, C.B., Lenihan, H.S.,
672 Pandolfi, J.M., Peterson, C.H., Steneck, R.S., Tegner, M.J., Warner, R.R., 2001. Historical
673 overfishing and the recent collapse of coastal ecosystems. *Science*, 293, 629–638.
- 674 Jenness, J., Brost, B., Beier, P. 2011. Land facet corridor designer: extension for ArcGIS. *Jenness*
675 *Enterprises*, Flagstaff.
- 676 Kruss, A, Blondel, Ph, Tegowski, J, 2012. Acoustic properties of mycophytes: comparison of
677 single-beam and multibeam imaging with modelling results. In: *11th European Conference on*
678 *Underwater Acoustics*, St. Albans: Institute of Acoustics, 168-175.
- 679 Lamarche, G, Lurton, X., Verdier, A.-L., Augustine, J.-M. 2011. Quantitative characterisation of
680 seafloor substrate and bedforms using advanced processing of multibeam backscatter –
681 Application to Cook Strait, New Zealand. *Continental Shelf Research*, 31, S93-S109.

- 682 Lecours, V., Dolan, M.F.G., Micallef, A., Lucieer, V. L. 20166 online. Characterising the ocean
683 frontier: A review of marine geomorphometry. *Hydrology and Earth system Sciences, Discussions*,
684 DOI:10.5194/hess-2016-73
- 685 Lucieer, V.L. 2007. The application of automated segmentation methods and fragmentation
686 statistics to characterise rocky reef habitat. *Journal of Spatial Science*, 52, 81-91.
- 687 Lucieer, V., Hill, N. A., Barrett, N. S., and Nichol, S., 2013. Do marine substrates “look” and “sound”
688 the same? Supervised classification of multibeam acoustic data using autonomous underwater
689 vehicle images. *Estuarine, Coastal and Shelf Science*, 117, 94-106.
- 690 Lucieer, V., Lamarche, G., 2011. Unsupervised fuzzy classification and object-based image
691 analysis of multibeam data to map deep water substrates, Cook Strait, New Zealand. *Continental*
692 *Shelf Research*, 31, 1236–1247.
- 693 Magri, O. 2006. A geological and geomorphological review of the Maltese Islands with special
694 reference to the coastal zone. *Territoris*, 6, 7-26.
- 695 Marsh, I. Brown, C. 2009. Neural network classification of multibeam backscatter and bathymetry
696 data from Stanton Bank (area IV). *Applied Acoustics*, 70, 1269-1276.
- 697 McGonigle C., Brown C., Quinn R., Grabowski J., 2009. Evaluation of image-based multibeam
698 sonar backscatter classification for benthic habitat discrimination and mapping at Stanton Banks,
699 UK. *Estuarine, Coastal and Shelf Science*, 81, 423–437
- 700 McGonigle, C., Collier, J., 2014. Interlinking backscatter, grain size and benthic community
701 structure. *Estuarine, Coastal Shelf Science*, 147, 123-136.
- 702 Micallef, A., Le Bas, T. P., Huvenne, V. A. I., Blondel, Ph., Hühnerbach, V. Deidun, A. 2012. A multi-
703 method approach for benthic habitat mapping of shallow coastal areas with high-resolution
704 multibeam data. *Continental Shelf Research*, 39-40, 14-26.

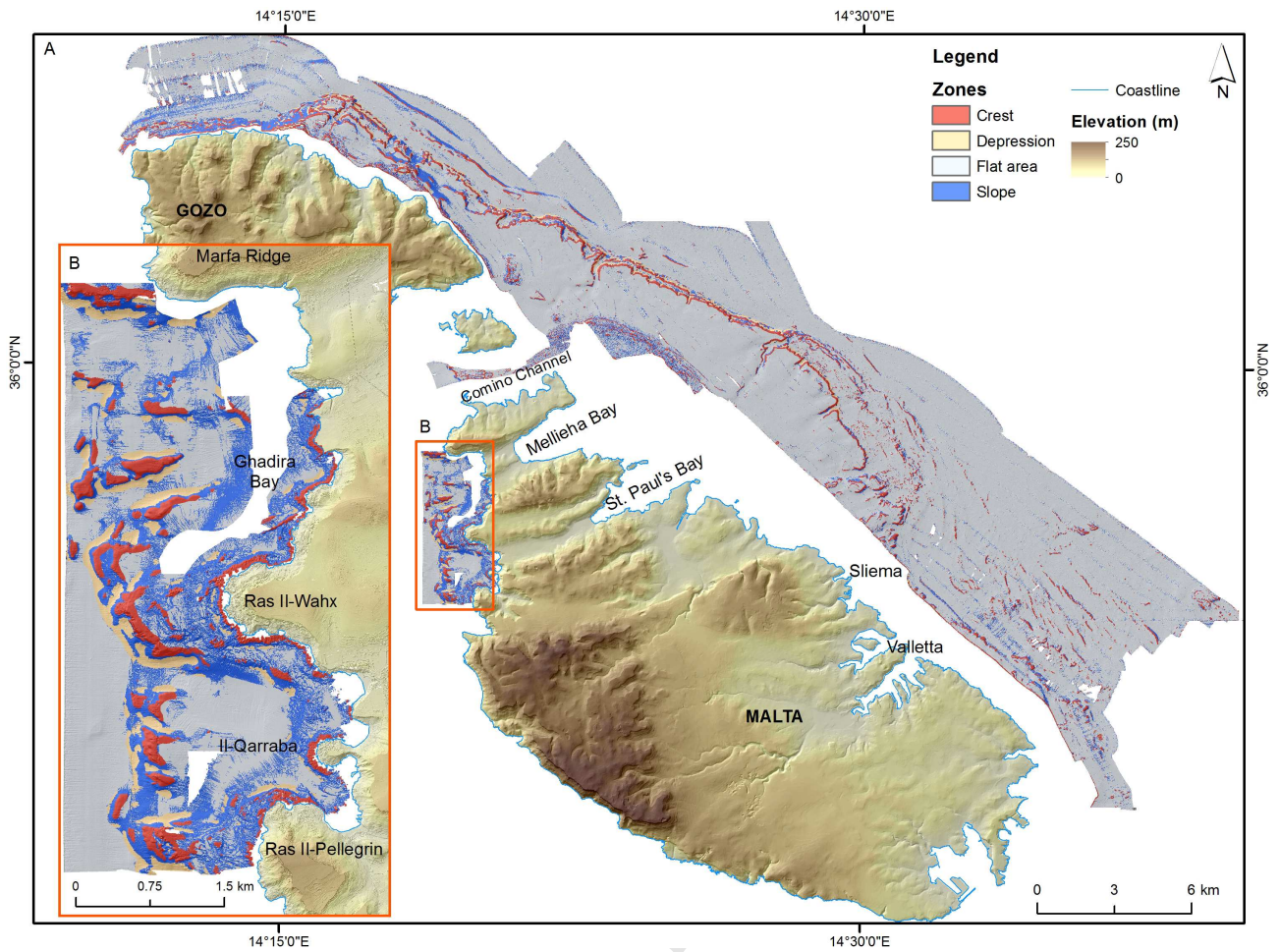
- 705 Micallef, A., Foglini, F., Le Bas, T., Angeletti, L., Maselli, V., Pasuto, A. Taviano, M. 2013. The
706 submerged paleolandscape of the Maltese Islands: morphology evolution and relation to
707 Quaternary environmental change. *Marine Geology*, 335, 129-147.
- 708 Montereale Gavazzi, G., Madricardo, F., Sigovini, M., Janowski, L., Kruss, A., Blondel, Ph., Foglini,
709 F. 2016. Evaluation of seabed mapping methods for fine-scale benthic habitat classification in
710 extremely shallow environments – Application to the Venice Lagoon, Italy. *Estuarine, Coastal and*
711 *Shelf Sciences*, 170, 45-60.
- 712 Pedley, M., Clarke, M. H. 2002. Limestone Isles in a Crystal Sea: the geology of the Maltese
713 Islands. *Publishers Enterprises Group*.
- 714 Pérès, J. M., 1985. History of the Mediterranean biota and the colonisation of the depths. In:
715 Margalef, R. (ed), *Western Mediterranean*, Pergamon Press, U.K., p. 198-232.
- 716 Preston J. M., Rosenberger A., Collin W. T., 2000. Bottom classification in very shallow water. *IEEE*
717 *Oceans'2000 Proceedings*, 3, 1563-1567.
- 718 Preston, JM., 2009. Automated acoustic seabed classification of multibeam images of Stanton
719 Banks. *Applied Acoustics*, 70(10), 1277–87.
- 720 Putz-Perrier, W. Sanderson, D. J. 2010. Distribution of faults and extensional strain in fractured
721 carbonates of the North Malta Graben. *AAPG Bulletin*, 9(4), 435–456
- 722 Rattray, A., Ierodiaconou, D., Laurensen, L., Burq, S., Reston M., 2009. Hydro-acoustic remote
723 sensing of benthic biological communities on the shallow South East Australian continental shelf.
724 *Estuarine, Coastal and Shelf Science*, 84, 237–245.
- 725 Rooper C. N., Zimmermann M., 2007. A bottom-up methodology for integrating underwater video
726 and acoustic mapping for seafloor substrate classification. *Continental Shelf Research*, 27, 947-
727 957,

- 728 Sciberras, M., Rizzo, M., Mifsud, J.R., Camilleri, K., Borg, J.A., Lanfranco, E. Schembri P.J. 2009.
729 Habitat structure and biological characteristics of a maerl bed off the northeastern coast of the
730 Maltese Islands (central Mediterranean). *Marine Biodiversity*, 39, 251–264.
- 731 Simons, D. G., Snellen, M., 2009. A Bayesian approach to seafloor classification using multi-beam
732 echo-sounder backscatter data. *Applied Acoustics*, 70, 1258–1268.
- 733 Verfallie, E., Doornenbal, P., Mitchell, A.J., White, J., Van Lancker, V., 2007. The bathymetric
734 position index (BPI) as a support tool for habitat mapping. Worked example for the MESH
735 Final Guidance, 14 pp.
- 736 Wright, D. J., Heyman, W. D., 2008. Introduction to the special issue: Marine and Coastal GIS for
737 Geomorphology, Habitat Mapping, and Marine Reserves. *Marine Geodesy*, 31(4), 223-230.
- 738 Wright, D. J., Lundblad, E. R., Larkin, E. M., Rinehart, R. W., Murphy, J., Cary-Kothera, L., and
739 Draganov, K., 2005. ArcGIS benthic terrain modeler. Oregon State University, Corvallis, OR, USA.
- 740 AquaBioTech Group – <https://www.aquabt.com/>
- 741 Malta Environment Planning Authority (MEPA) – www.mepa.org.mt
- 742 SWATHplus-L – www.sea.co.uk/products/survey/SWATHplus.aspx
- 743 Global Offshore Wind Farm Database – [http://www.4coffshore.com/windfarms/sikka-l-bajda-malta-](http://www.4coffshore.com/windfarms/sikka-l-bajda-malta-mt01.html)
744 [mt01.html](http://www.4coffshore.com/windfarms/sikka-l-bajda-malta-mt01.html)
- 745 Physical Oceanography Online – <http://ioi.research.um.edu.mt/capemalta/stations@malta/INDEX/>
- 746
- 747
- 748
- 749
- 750

751 **FIGURE CAPTIONS**

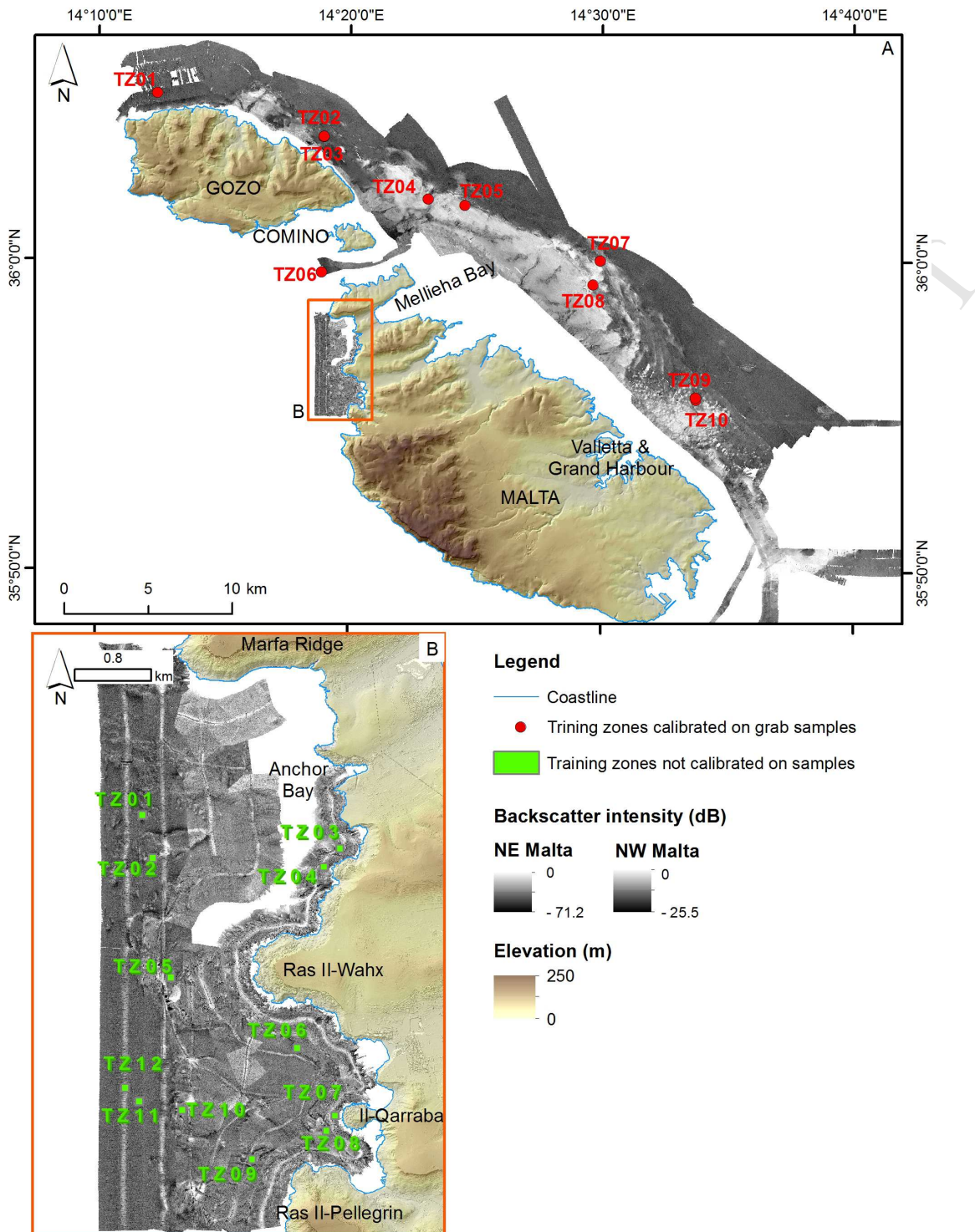
752

753 **Figure 1.** Geology and acquired bathymetry of the Maltese archipelago. Geographical and
 754 geological setting of the Maltese archipelago (see text for references about geology) and new high-
 755 resolution (2 m) bathymetry of the study area, acquired with SWATHplus-L (NW coast of Malta)
 756 and Kongsberg EM710 (E coasts of the Maltese Islands). The main faults are highlighted in brown,
 757 showing the WSW-ENE system and the NW-SE orientations parallel to the Pantelleria Rift, further
 758 offshore west of Malta.



759

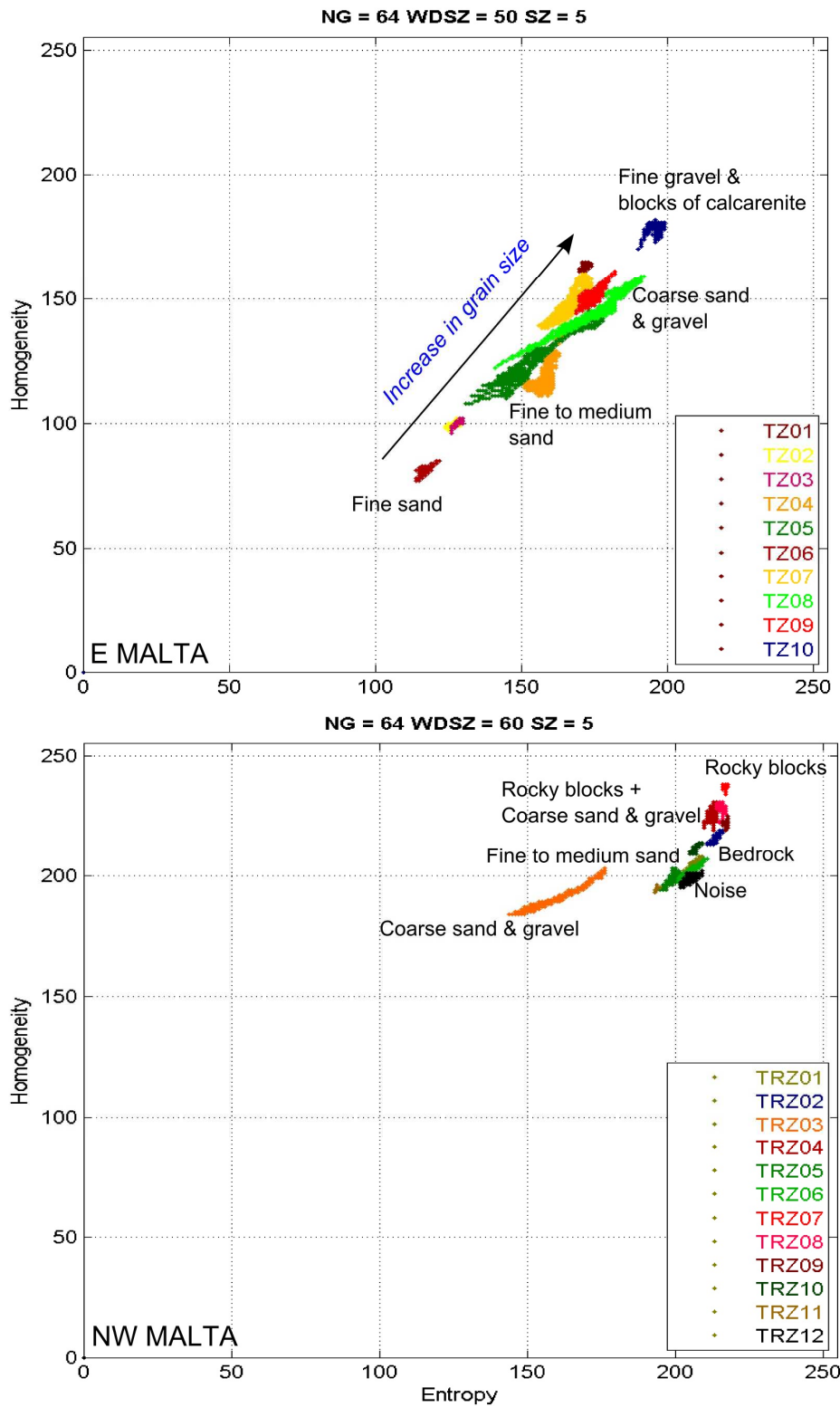
760 **Figure 2.** Seafloor morphological classification, related to land topography of the Maltese Islands.
 761 Maps obtained with the Benthic Terrain Modeler (BTM) toolbox of ArcGIS 10.x (Wright and
 762 Heyneman, 2005). A) Global overview of all areas; B) Details of the NW Malta dataset, showing a
 763 clearly more complex morphology.



764

765 **Figure 3.** A) Backscatter of the area located offshore the eastern coasts of the Maltese
 766 archipelago and B) of the area offshore the NW coast of the Island of Malta. Note the grey level
 767 scales are slightly different, to better emphasize local features. Training Zones for the E dataset
 768 are defined around grab samples at coinciding locations (red circles). Training Zones for the NW

769 dataset are not based on grab samples and are represented as green squares. Onshore elevation
 770 data from 0 to 250 m.

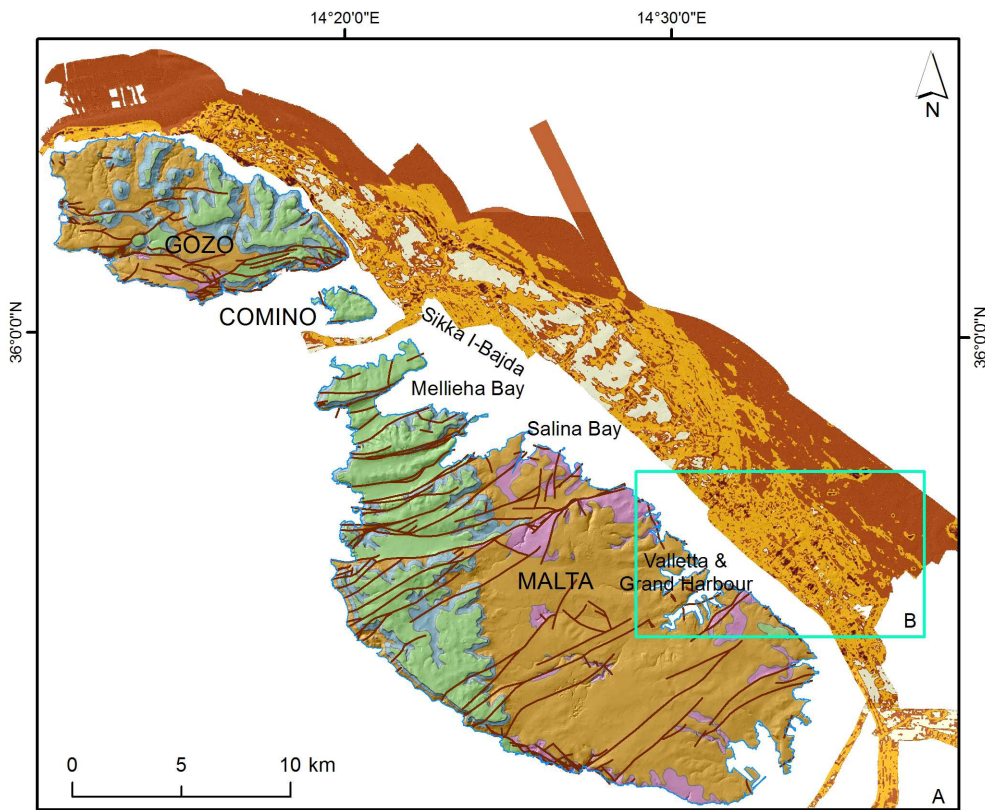


771

772 **Figure 4.** Entropy/homogeneity distributions of Training Zones of both datasets. Textures have
 773 been tested on a large number of Training Zones (10 for the E Malta dataset, 12 for the NW Malta

774 dataset), defined as representative of the different acoustic facies (Tables A1 and A2 respectively)
775 and associated to grab samples for the E dataset. Entropy and homogeneity were computed on
776 backscatter images resampled onto 64 grey levels (NG), with moving windows of similar sizes
777 (WDSZ = 50 and 60 pixels respectively) and looking at co-occurrences 5 pixels away (SZ). Top
778 (NE Malta): the clear separation of training zones shows a progression in entropy and homogeneity
779 associated to increasing grain sizes, with more sedimented areas at the bottom-left part of the plot
780 and the more rocky areas at the top right. Bottom (NW Malta): the same progression is seen, with
781 smaller variations in homogeneity but similar variations in entropy. This is explained by differences
782 in the local geology (see text for details).

783

**Legend**

— Coastline

— Fault

Geology

Upper Coralline Limestone Fm.

Blue Clay Fm.

Globigerina Limestone Fm.

Lower Coralline Limestone Fm.

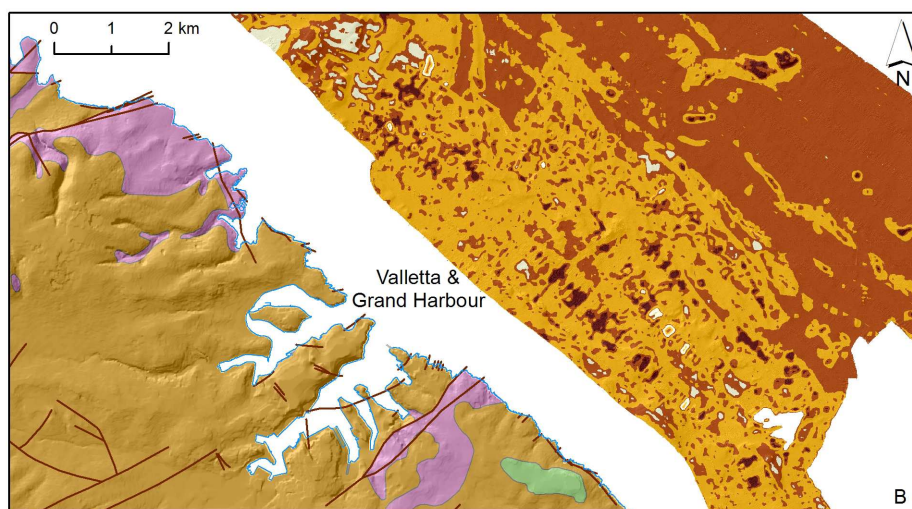
Seafloor sediment

Bedrock

Coarse sand & gravel

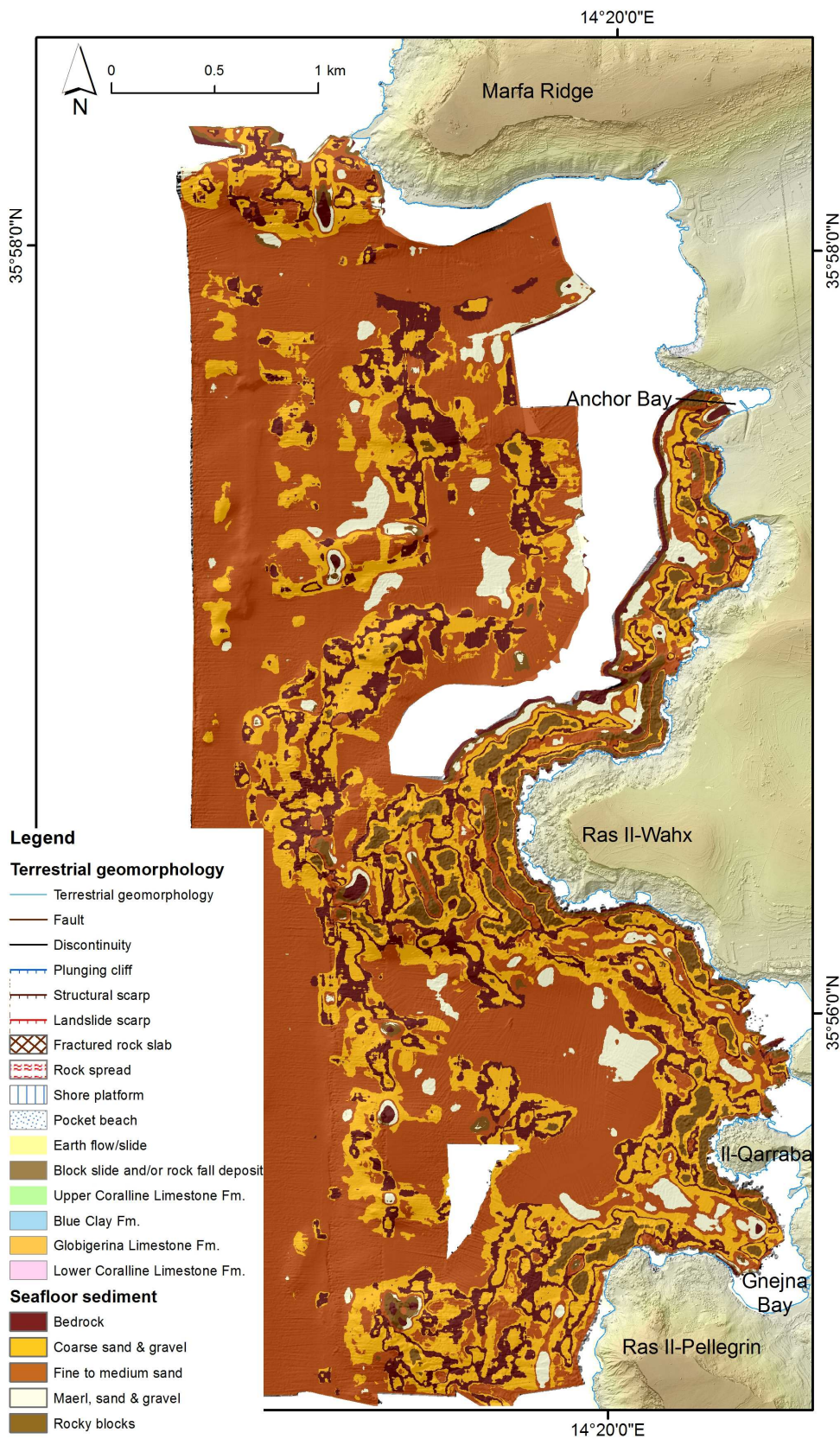
Fine to medium sand

Maerl, sand & gravel



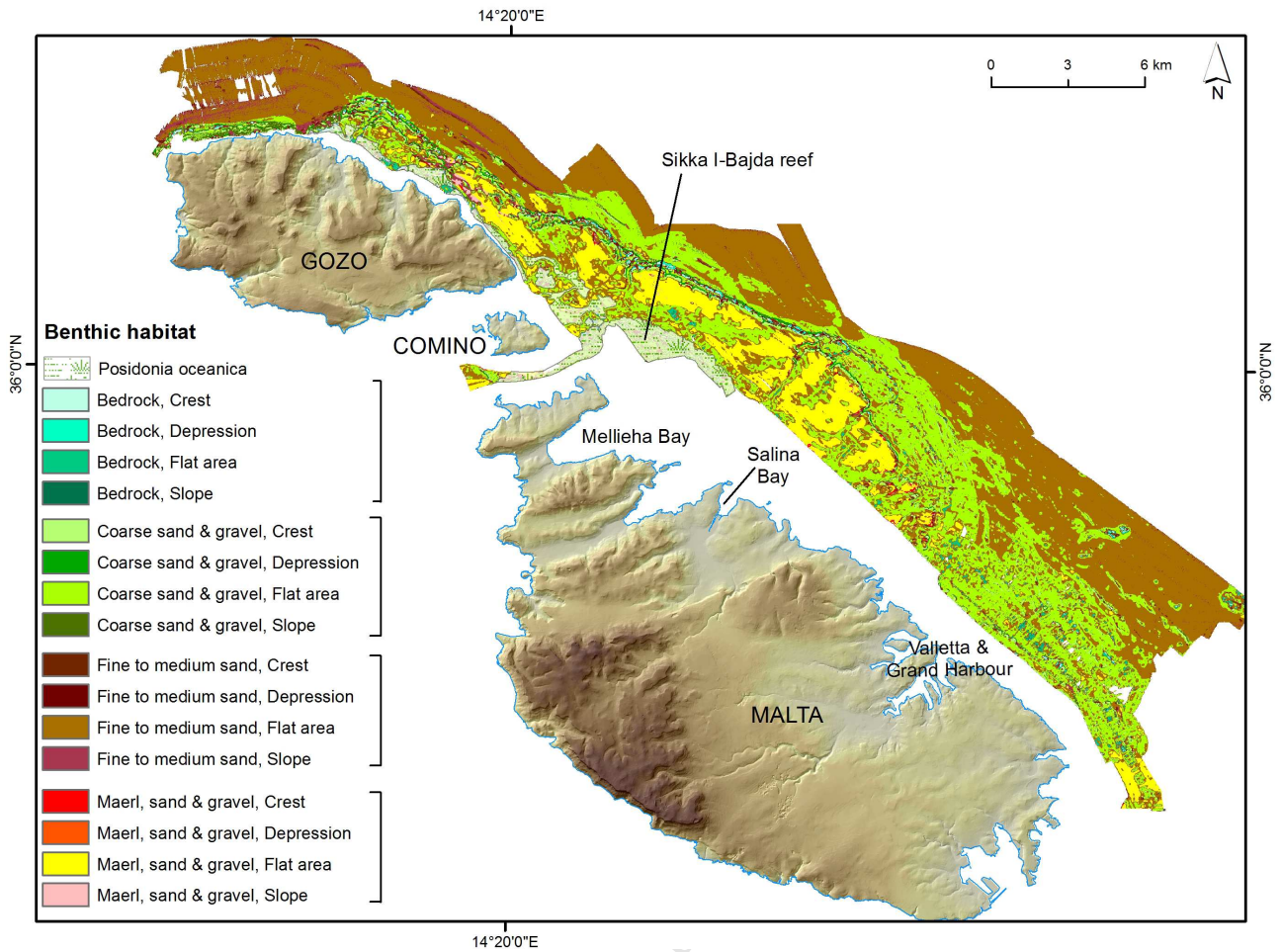
784

785 **Figure 5.** A) Seafloor sediment maps derived from TexAn classification – E Malta dataset. B) Detail
 786 of theseafloor offshore Valletta and the Grand Harbour affected by anthropogenic activities.



787

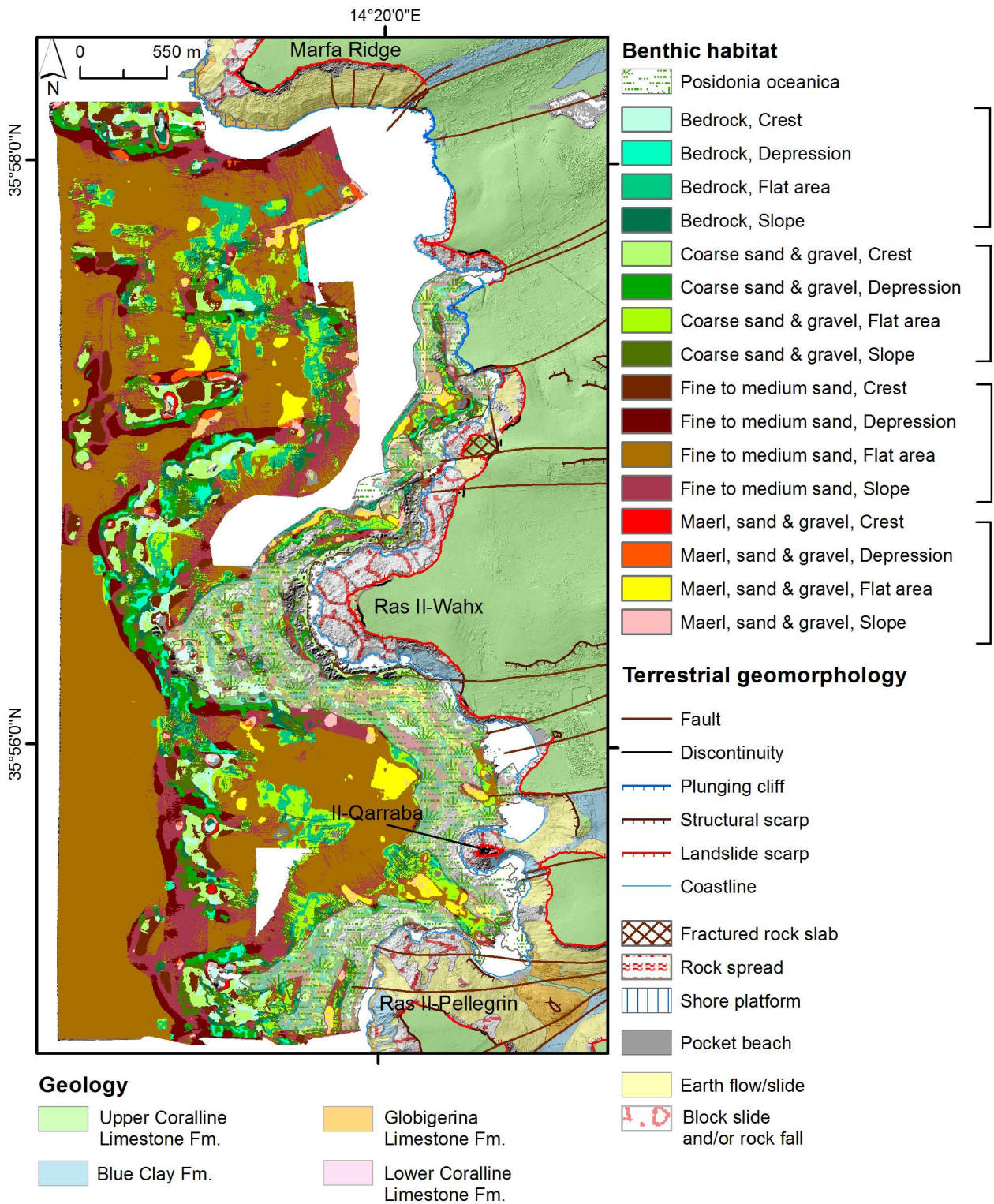
788 **Figure 6.** Benthic habitat map for the E Malta dataset derived from the combination of BTM (Figure
 789 2) and Texan (Figure 5) classifications, combined with available MEPA information on *Posidonia*
 790 *oceanica* and *maërl* distribution.



791

792 **Figure 7.** Seafloor sediment maps derived from TexAn classification – NW Malta dataset. The
 793 continuation of terrestrial geomorphology (modified from Devoto et al. 2012) on the seafloor is
 794 highlighted.

795




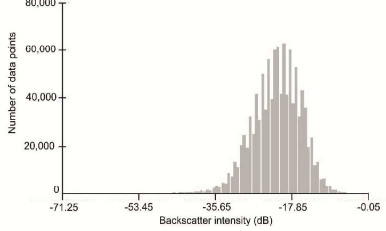
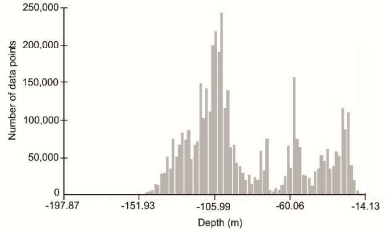

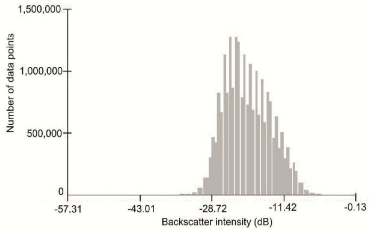
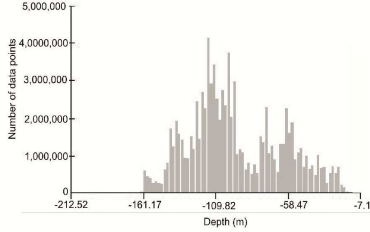

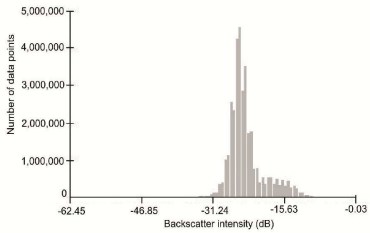
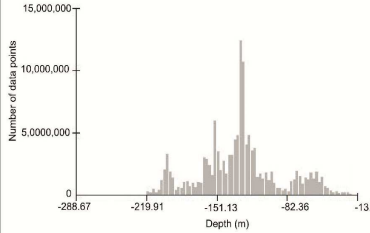
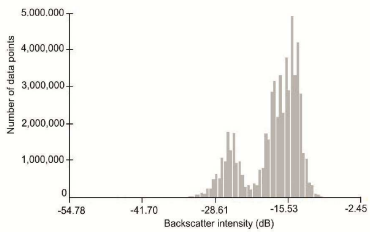
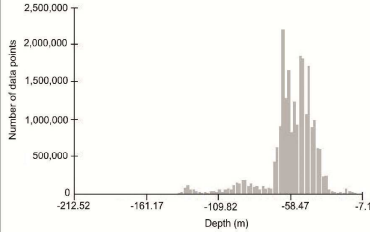
796

797 **Figure 8.** Benthic habitat map for the NW Malta dataset derived from the combination of BTM
 798 (Figure 2) and Texan (Figure 5) classifications, combined with available MEPA information on
 799 *Posidonia oceanica* distribution.

800

801 **TABLE CAPTIONS**

802 **Table 1.** Comparison of backscatter intensity values and bathymetric distribution of each sediment
 803 class for the E dataset.

Sediment class	Backscatter image	Backscatter histogram	Bathymetry histogram	Notes
Bedrock				Characterised by high values of backscatter intensity and including different type of patterns, this class is located mainly in two bands of depth: from shallow waters to 690 m deep (where some positive reliefs occur) and from 80 to 130 m deep (corresponding to the shelf break).
Coarse sand & gravel				Characterised by slightly lower backscatter than bedrock class, it is more uniformly distributed down to a depth of about 160 m.
Fine to medium sand				Characterised by a frequency peak around -25 dB, it is distributed mainly in deeper areas with a peak at ca. 130 m deep.
Maërl, sand & gravel				Occurring mainly on the continental shelf, down to ca. 70 m deep, it is characterised by two modes of backscatter intensity.


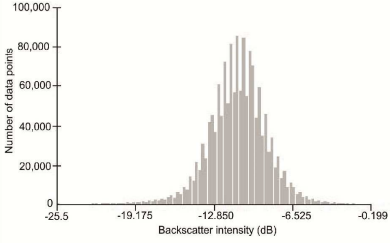
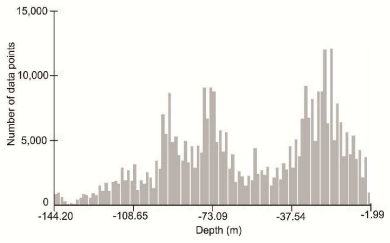

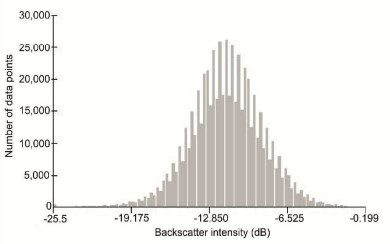
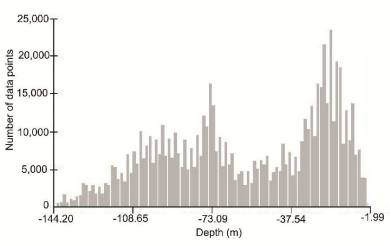

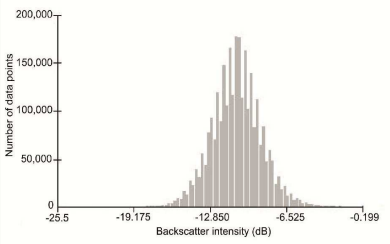
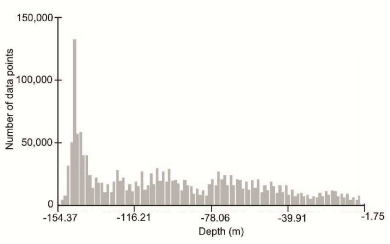

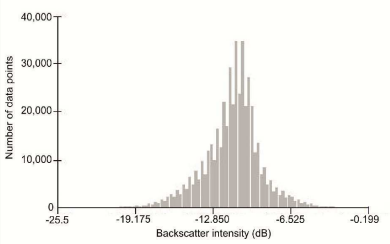
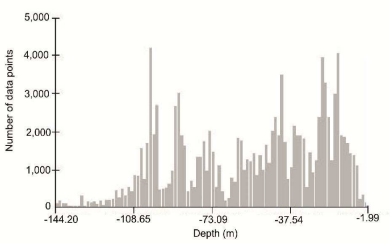

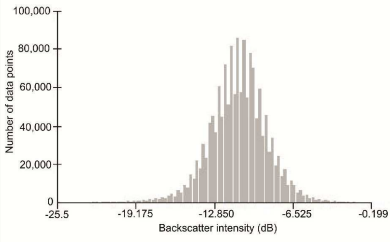
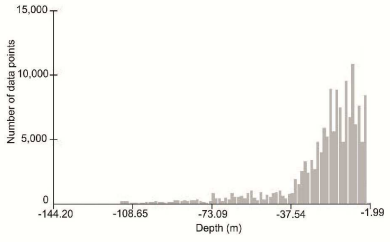
804

805

806

807

808 **Table 2.** Comparison of backscatter intensity values and bathymetric distribution of each sediment
 809 class for the NW dataset.

Sediment class	Backscatter image	Backscatter histogram	Bathymetry histogram	Notes
Bedrock				The bedrock class is present mainly near-shore and between 70 and 90 m deep (the latter representing the shelf break). The characteristic backscatter intensity shows the same distribution as the intensity of the entire dataset.
Coarse sand & gravel				Two main areas of the seafloor are made up of coarse sand and gravel: one in shallow water (maximum depth of about 38 m) and the other between ca. 70 and 105 m deep. The backscatter intensity is more centred on the medium values of the dataset.
Fine to medium sand				It is present in the whole dataset, especially in deep waters (> 118 m). The majority of intensity values between ca. -8 and -10 dB characterises this sediment class.
Maërl, sand & gravel				It is generally widespread at all depths with the exception of deep waters (> 110 m). The predominant backscatter intensity within this class is medium (from ca. -13 to -8 dB).
Rocky blocks				Class located mainly in shallow water (maximum depth of ca. 37 m). The backscatter intensity distribution is Gaussian: predominantly medium values of intensity but with low number of records.

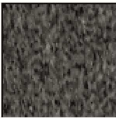
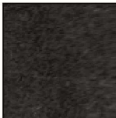

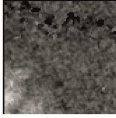


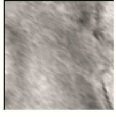

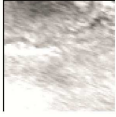
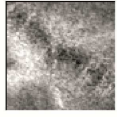
810

811

812

813 **SUPPLEMENTARY MATERIAL CAPTIONS**

814 **Table A1.** Training Zones of the E mosaic, 80 x 80 pixels (i.e. 160 x 160 m on the ground), with
 815 associated description of the sample centred in the Training zone, the type of sediment (from grain-
 816 size analyses) and seabed composition (from the entropy/homogeneity diagram).

NAME	MOSAIC	SAMPLES	SEDIMENT TYPE	TEXAN CLASSIFICATION	NAME	MOSAIC	SAMPLES	SEDIMENT TYPE	TEXAN CLASSIFICATION
trz01		MEDCORE 40 TOP	Very well sorted fine sand	Fine to medium sand	trz06		DECORS 45 TOP	Muddy fine sand	Fine to medium sand
trz02		MEDCORE 51 TOP	Fine sand; Posidonia leaves and rhizomes	Maërl sand & gravel	trz07		MARCOS 77 TOP	Muddy fine sand & gravel	Coarse sand & gravel
trz03		MEDCORE 42 TOP	Coarse sand; Posidonia leaves and rhizomes	Maërl sand & gravel	trz08		DECORS 47	Medium sand; Maërl	Coarse sand & gravel
trz04		MEDCORE 57 TOP	Gravelly fine sand	Fine to medium sand	trz09		MEDCORE 60 TOP	Muddy fine sand	Fine to medium sand
trz05		MARCOS 76	Muddy coarse sand	Coarse sand & gravel	trz10		MEDCORE 59	Fine gravel; Blocks of calcarenite (ø 5-20cm)	Coarse sand & gravel

817

818

819

820


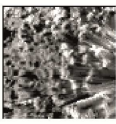
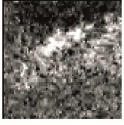







821

822

823

824

825 **Table A2.** Training Zones of the NW mosaic, 82 x 82 pixels (i.e. 82 x 82 m on the ground), with
 826 associated description of backscatter and morphology, and the seabed composition (from the
 827 entropy/homogeneity diagram).

NAME	MOSAIC	DESCRIPTION	TEXAN CLASSIFICATION	NAME	MOSAIC	DESCRIPTION	TEXAN CLASSIFICATION
TZ01		Area downslope the escarpment with a block (ø 69x54 m; height 11 m) buried under medium-fine sediment.	Fine to medium sand; Coarse sand & gravel	TZ07		Really close to the coast, sloping area characterised by numerous, not spatially organised, blocks (ø 13x16 m; 12x17 m; 12x14 m; height 1-2-5 m)	Rocky blocks; Bedrock; Coarse sand & gravel
TZ02		Area downslope the escarpment. Presence of a break of slope oriented ENE-WSW (height 21 m; mean slope 30°)	Coarse sand & gravel; Bedrock	TZ08		Flat and smooth area, close to the coast, located immediately downslope the accumulation of blocks accumulation (mosaic TZ07, above). Presence of acoustic imaging artefacts (a few straight lines).	Rocky blocks; Coarse sand & gravel
TZ03		Area close to the coast, flat, generally smooth and with variation of sedimentary coverage	Rocky blocks; Fine to medium sand; Coarse sand & gravel	TZ09		Generally flat area, presence of some blocks (ø 10x8 m, 12x14 m, 8x8 m; height 40cm, 1 m, 3 m)	Rocky blocks; Coarse sand & gravel
TZ04		Area close to a promontory, presence of blocks (27x17 m; 14x17 m; 10x18 m; height 3-5 m).	Bedrock; Rocky blocks; Coarse sand & gravel	TZ10		Area characterised by irregular, N-S oriented continental escarpment (40-50° sloping and 20 m high)	Bedrock; coarse sand & gravel
TZ05		Shelf area, flat and quite smooth, interpreted as palaeo-shore platform. Presence of artefacts.	Fine to medium sand	TZ11		Flat and smooth area with some imaging artefacts (faint horizontal lines).	Fine to medium sand

828

829

830

831

832

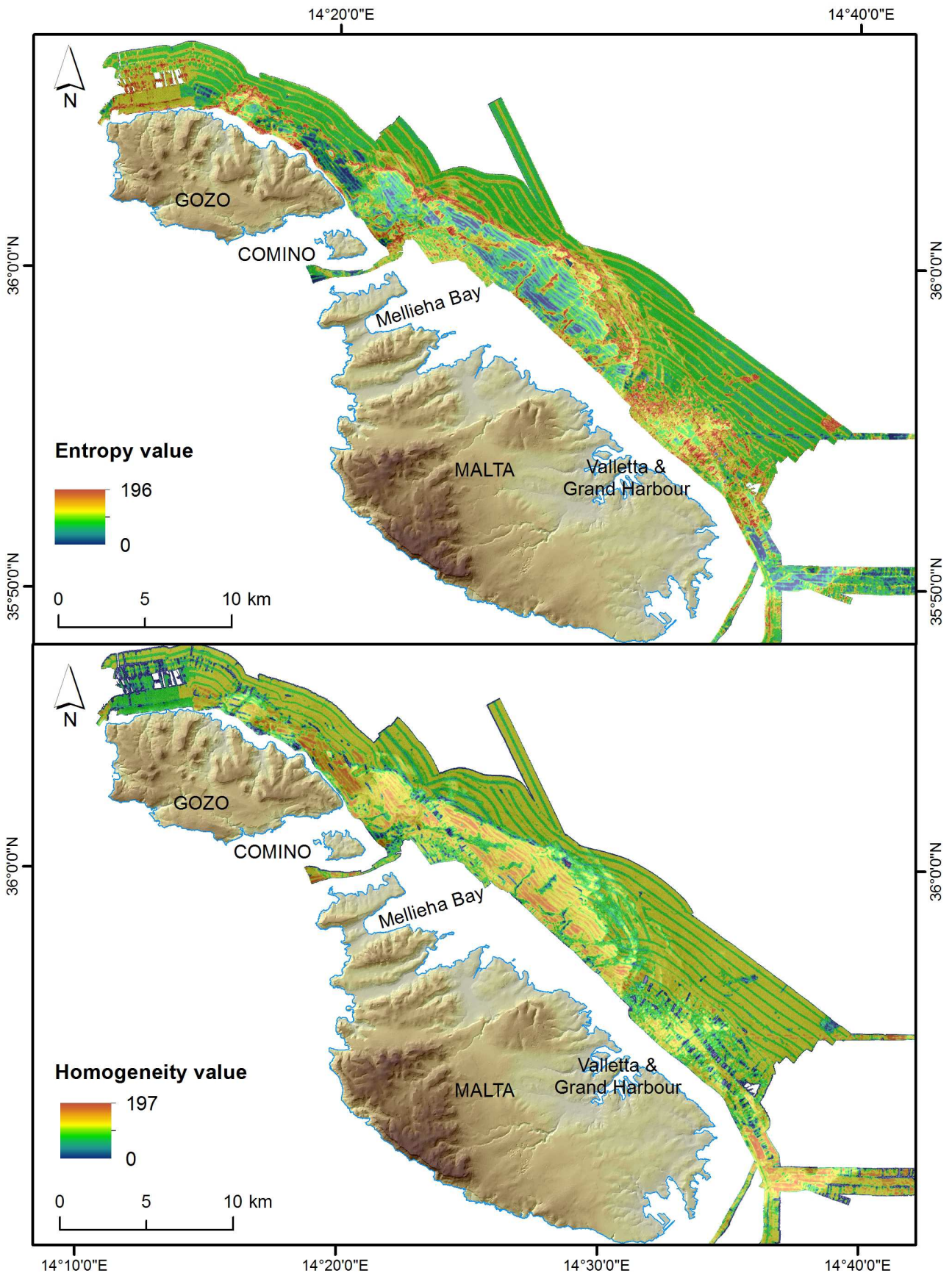
833

834

835

836

837

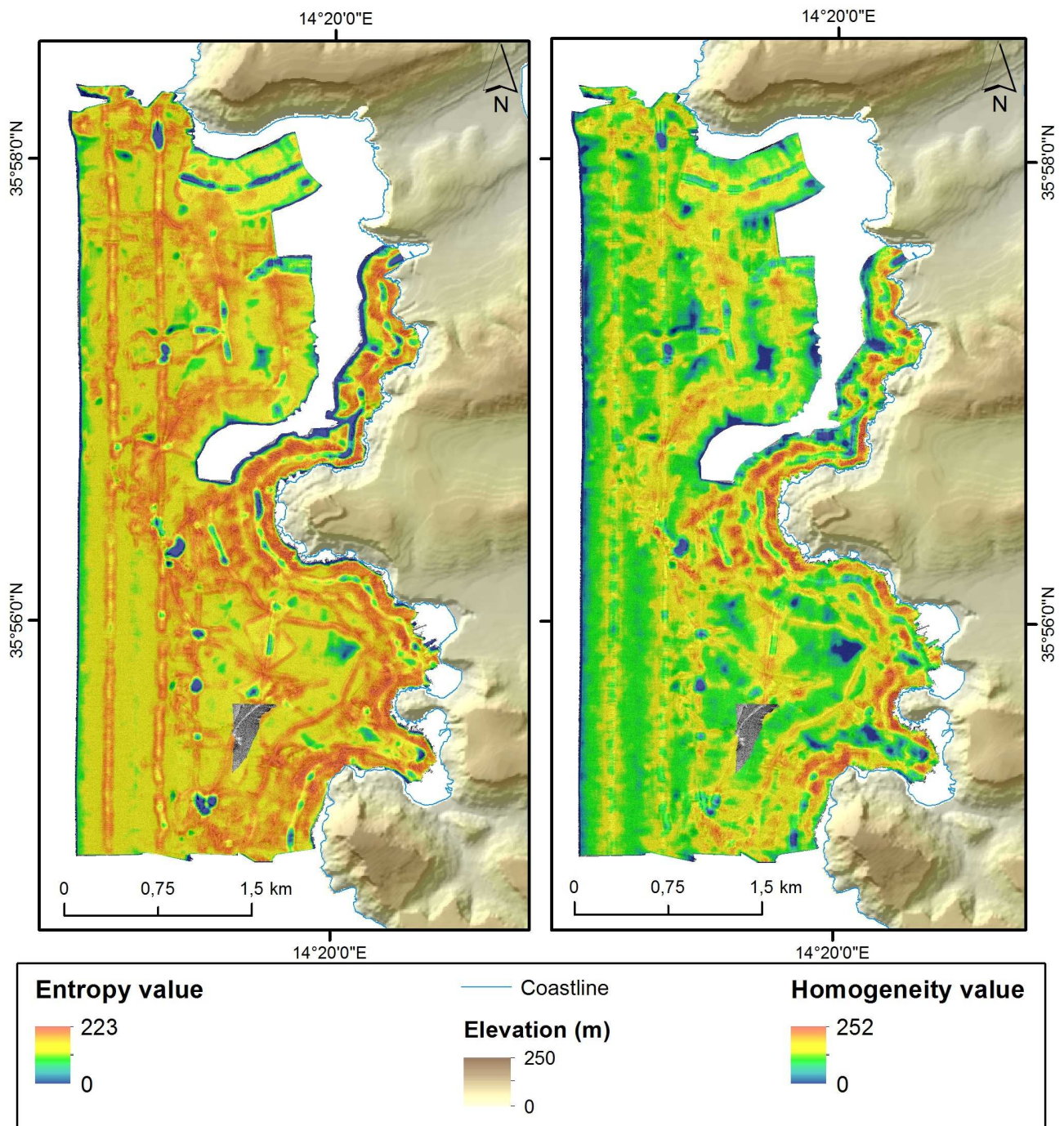


838

839 **Figure A1.** Entropy and homogeneity maps for the E Malta dataset. The square shows a detail of
840 the bottom of the palaeo-river channels and of the variations of entropy and homogeneity values

841 inside the channels. Entropy and homogeneity distributions obtained from the TexAn processing of
842 the whole E dataset show similar characteristics. The navigation lines are very visible and
843 characterised by high entropy and low homogeneity values, but they are easily removed later,
844 during the K-means classification. Generally, the basin area presents an almost homogeneous
845 seafloor, with medium entropy and homogeneity. The continental escarpment, characterised by
846 high backscatter intensity, is highlighted by high values of entropy and low values of homogeneity,
847 representing an important passage from two different environments (the basin and the continental
848 shelf). We can observe the same for the area characterised by the ridges of the palaeo-shoreline
849 deposits. The continental shelf shows high variations of entropy and homogeneity values: the
850 platform is generally homogeneous in substrate type, but it is characterised by some highly
851 heterogeneous features. The bottoms of the palaeo-river valleys show high entropy and low
852 homogeneity, and their uppermost parts are more marked than their mouths. This mixed area is
853 due to the variations in sediment type characterising the bottom of the channels and similar to a
854 pattern typical of ripples. Also the shallow area offshore Comino and Mellieha Bay shows high
855 values of entropy and low homogeneity. Another interesting zone is the seafloor in shallow water
856 offshore Valletta: its shows a dotted distribution of high and medium values of entropy and
857 homogeneity, explained further in this section.

858



860 **Figure A2.** Entropy and homogeneity maps for the NW Malta dataset, showing details of the area.
 861 Entropy measures textural roughness, and homogeneity is lower as textures are more organised.
 862 Both parameters are visibly sensitive to artefacts introduced at the junction between swaths; this
 863 was accounted for in the selection of Training Zones (Table A2) and the classification of
 864 entropy/homogeneity signatures. The maps show a continental shelf characterised by high
 865 variations in entropy and homogeneity values. On the contrary, the area located downslope the
 866 continental escarpment is characterised by medium values of both indices, without variations in

867 intensity, reflecting an almost homogeneous backscatter image, apart from the noisy track lines,
868 highlighted by high entropy and high homogeneity values. The boundaries of the plateau offshore
869 Ghadira Bay are highlighted by values of entropy and homogeneity both higher than the
870 surroundings. Generally, the edges between individual swaths are marked with high entropies and
871 high homogeneities, identified and removed during the next stage.

872

ACCEPTED MANUSCRIPT

Highlights

1. Multi-method approach was applied for benthic habitat mapping of Maltese seafloor
2. We combined morphometric and TexAn analyses of sonar image
3. The classifications were compared with those already available in literature
4. We produced comparable classifications of datasets acquired with different devices

ACCEPTED MANUSCRIPT